Probabilistic models for computational stochastic mechanics and applications

Christian Soize

▶ **To cite this version:**

Christian Soize. Probabilistic models for computational stochastic mechanics and applications. 9th International Conference on Structural Safety and Reliability ICOSSAR'05, Rome, Italy, 19–23 June 2005, Jun 2005, Rome, Italy. pp.23-42 (Plenary Lecture). hal-00687868

HAL Id: hal-00687868
https://hal.science/hal-00687868

Submitted on 15 Apr 2012

HAL is a multi-disciplinary open access archive for the deposit and dissemination of scientific research documents, whether they are published or not. The documents may come from teaching and research institutions in France or abroad, or from public or private research centers.

L'archive ouverte pluridisciplinaire **HAL**, est destinée au dépôt et à la diffusion de documents scientifiques de niveau recherche, publiés ou non, émanant des établissements d'enseignement et de recherche français ou étrangers, des laboratoires publics ou privés.

Probabilistic models for computational stochastic mechanics and applications

C. Soize
University of Marne-la-Vallée, Paris, France

Keywords: comptational stochastic mechanics, model uncertainties, data uncertainties, dynamical systems

ABSTRACT: This paper deals with the validation and industrial applications of a nonparametric probabilistic approach of model uncertainties and data uncertainties in computational dynamics for linear and nonlinear dynamical systems, for complex structures and vibroacoustic systems. First, data uncertainties and model uncertainties in a predictive model of a real system are defined. Then, the concept of the nonparametric probabilistic approach for random uncertainties due to model errors and data errors is introduced. A short overview of the main theoretical results of this nonparametric approach based on the use of ensembles of random matrices constructed with the maximum entropy principle is given. The methodology of this nonparametric probabilistic approach is given. A numerical validation proving the capability of the nonparametric probabilistic approach to take into account model uncertainties is presented. Then an experimental validation is given for the dynamics of a composite sandwich panel. Finally, four industrial applications of the nonparametric probabilistic modeling of random uncertainties in comptational stochastic mechanics for complex mechanical systems are presented: (1) The linear dynamics of a bladed disk mistuned due to manufacturing tolerances uncertainties; (2) The identification and quantification of the design margins in the nonlinear dynamics of a reactor coolant system; (3) The robustness of the numerical simulation model with respect to model and data uncertainties in dynamics of a spatial structure; (4) The robustness of the numerical vibroacoustic FRF of cars with respect to model and data uncertainties.

1 INTRODUCTION

The treatment of data uncertainties in structural mechanics has received a considerable attention these last decades. Data uncertainties affect the parameters of the mathematical-mechanical model such as the dimensions parameters, the parameters allowing the boundary conditions to be described, the constitutive equations, etc. Data uncertainties can clearly be taken into account by the parametric probabilistic approach. Such probabilistic analysis of data uncertainties performed with random variables modeling for relatively simple mechanical system can be found in many papers such as Shinozuka & Astill (1972), Chen & Soroka (1973), Prasthofer & Beadle (1975), Haug et al. (1986), Ibrahim (1987), Kotulski ans Sobczyk (1987), Shinozuka (1987), Jensen & Iwan (1992), Iwan & Jensen (1993), Lee & Singh (1994), Papadimitriou et al. (1995), Lin & Cai (1995), Micaletti et al. (1998), Schuëller (1997), Mignolet et al. (1998). Such a parametric probabilistic approach has also been developed with random field theory for data uncertainties and random media modeling, leading to the stochastic finite element method; see for instance Vanmarcke & Grigoriu (1983), Liu et al. (1986), Shinozuka & Deodatis (1988), Spanos & Ghanem (1989), Ghanem & Spanos (1991), Kleiber et al. (1992), Spanos and Zeldin (1994), Ditlevsen & Tarp-Johansen (1998). More recently, the parametric probabilistic approach for data uncertainties and for random media has been developed and applied to the computational mechanics of large and complex mechanical systems; see for instance Hien & Kleiber (1997), Ghanem & Dham (1998), Ghanem (1999), Székely & Schuëller (2001), Le Maître et al (2001) and (2002), Pradlwarter et al. (2002), Schuëller et al. (2003), Schenk & Schuëller (2003).

This paper does not deal with the above parametric probabilistic approach for data uncertainties or stochastic finite element method for random media, but rather with a nonparametric probabilistic approach of model uncertainties and data uncertainties for computational stochastic dynamics. This approach has been introduced by Soize (1999) and developed in the last five years. The main objectif of this paper is to present new validations of this approach and

industrial applications in several fields for complex mechanical systems in computational stochastic mechanics for linear and nonlinear dynamical systems, for structural dynamics and vibroacoustic problems.

Notation. In this paper, $\mathbb{M}_n(\mathbb{R})$, $\mathbb{M}_n^S(\mathbb{R})$ and $\mathbb{M}_n^+(\mathbb{R})$ are the set of all $(n \times n)$ real matrices, the set of all symmetric $(n \times n)$ real matrices, and the set of all positive-definite symmetric $(n \times n)$ real matrices, respectively. We have $\mathbb{M}_n^+(\mathbb{R}) \subset \mathbb{M}_n^S(\mathbb{R}) \subset \mathbb{M}_n(\mathbb{R})$. If $[A]$ belongs to $\mathbb{M}_n(\mathbb{R})$, $\|[A]\|_F = (\mathrm{tr}\{[A]\,[A]^T\})^{1/2}$ is the Frobenius norm of matrix $[A]$, where tr is the trace of the matrices, det is the determinant of the matrices and $[A]^T$ is the transpose of matrix $[A]$. The operator norm of a matrix $[A] \in \mathbb{M}_n(\mathbb{R})$ is defined as $\|A\| = \sup_{\|\mathbf{x}\|\leq 1} \|[A]\,\mathbf{x}\| \quad , \quad \mathbf{x} \in \mathbb{R}^n$ and is such that $\|[A]\,\mathbf{x}\| \leq \|A\|\,\|\mathbf{x}\|\,, \forall \mathbf{x} \in \mathbb{R}^n$. The indicatrix function $\mathbb{1}_{\mathcal{B}}(b)$ of any set $\mathcal{B}$ is such that $\mathbb{1}_{\mathcal{B}}(b)$ is equal to 1 if $b \in \mathcal{B}$ and is equal to zero if $b \notin \mathcal{B}$. All random variables are defined on a probability space $(\mathcal{A}, \mathcal{T}, \mathcal{P})$ and E is the mathematical expectation.

2 DATA UNCERTAINTIES AND MODEL UNCERTAINTIES IN A PREDICTIVE MODEL OF A REAL SYSTEM

2.1 *Designed system*

In the context of engineering mechanics, the designed system is the mechanical system conceived by the designers and analysts. A designed system is defined by geometrical parameters, by the choice of materials, and by many other parameters. A designed system can be a very simple mechanical system e.g. an elastic bar or a very complex one such as an aircraft.

2.2 *Real system*

A real system is a manufactured version of a system realized from the designed system. Consequently, a real system is a man-made-physical system which is never exactly known (for instance, the geometry does not exactly coincide with the geometry of the designed system). A real system has then to be considered as an uncertain system with respect to the designed system. Uncertainties do not only affect the geometry, but also the boundary conditions, the materials, the mass density distribution, etc.

2.3 *Mean model as a predictive model: Errors and uncertainties*

The objective of a predictive model is to predict the output $\mathbf{v}^{\mathrm{exp}}$ of a real system to a given input $\mathbf{f}^{\mathrm{exp}}$. For instance, a predictive model can be developed for the static displacement field of a system subjected to a given external static load or, for the transient displacement field of a dynamical system subjected to an external impulsive load induced by a shock. Such predictive models are constructed by developing mathematical-mechanical model of the designed system for a given input (see Fig. 1). Consequently, the mean model has an input $\underline{\mathbf{f}}$ modeling $\mathbf{f}^{\mathrm{exp}}$, an output $\underline{\mathbf{v}}$ modeling $\mathbf{v}^{\mathrm{exp}}$ and exhibits a parameter $\underline{\mathbf{s}}$ for which data has to be given (it should be noted that the parameter can be a real number, a real vector, a real function, a field, a vector-valued function, etc.).

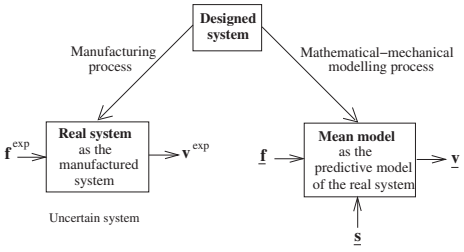

Figure 1. Designed system, real system and mean model as the predictive model of the real system.

(A) *Errors*: The errors are related to the construction of an approximation $\underline{\mathbf{v}}^n$ of the output $\underline{\mathbf{v}}$ of the mean model for given input $\underline{\mathbf{f}}$ and parameter $\underline{\mathbf{s}}$. For instance, if the mean model is a boundary value problem (BVP) defined on a bounded domain, the use of the finite element method for constructing a n-dimensional approximation space of the BVP solution introduces an error $\|\underline{\mathbf{v}} - \underline{\mathbf{v}}^n\|$ related to the finite element mesh size, where $\|\cdot\|$ is an appropriate norm. If a dynamical problem is studied, the use of a time integration scheme introduces an additional error related to the time sampling and to the time step. These errors are related to the construction of an approximate solution of the BVP and consequently, have to be reduced and controled using adapted methods developed in applied mathematics and in numerical analysis. In general, these errors must not be considered as uncertainties (see below).

(B) *Uncertainties*: Below, the input $\underline{\mathbf{f}}$ and the parameter $\underline{\mathbf{s}}$ of the mean model will be hereafter referred to as the data of the mean model. The mathematical-mechanical modeling process of the designed system introduces two fundamental types of uncertainties: the data uncertainties and the model uncertainties.

(B.1) *Data uncertainties*: The input $\underline{\mathbf{f}}$ of the mean model does not exactly represent the input $\mathbf{f}^{\mathrm{exp}}$ of the real system and there are also uncertainties on the parameter $\underline{\mathbf{s}}$ of the mean model. For instance, a static load represented by a point force is an approximation of the reality; the use of a given value of the Young modulus for a given elastic material is not an exact value (which is unknown), but corresponds to an uncertain value; the elastic constants of a complex joint between two substructures are uncertain, etc. Data uncertainties have to be taken into account for improving the predictability of the mean model. The best approach to take into account data uncertainties is the parametric probabilistic approach consisting in modeling the data of the mean model by random quantities (see Section 1).

© 2005 Millpress, Rotterdam, ISBN 90 5966 040 4

(B.2) *Model uncertainties*: The mathematical-mechanical modeling process used for constructing the mean model induces model uncertainties with respect to the designed system. This type of uncertainties is mainly due to the introduction of simplifications in order to decrease the complexity of the mean model which is constructed. For instance, a slender cylindrical elastic medium will be modeled by using the beam theory (such as an Euler or a Timoshenko beam), a thick rectangular plate elastic medium will be modeled by a thick plate theory (such as the Midlin plate theory), a complex joint constituted of an assemblage of several plates attached together by lines of bolts will be modeled by an equivalent homogeneous orthotropic plate, etc. It is clear that the introduction of such simplified models yields a mean model whose variations of parameter $\underline{\mathbf{s}}$ do not allow the model uncertainties to be reduced. Model uncertainties have to be taken into account to improve the predictability of the mean model. As explained above, the parametric probabilistic approach cannot be used (this point will be revisited in Section 5). This is the reason why a nonparametric probabilistic approach is proposed.

(C) *Predictability of the mean model*: The error between the prediction $\underline{\mathbf{v}}^n$ calculated with the mean model and the response $\mathbf{v}^{\exp}$ of the real system can be measured by $\|\mathbf{v}^{\exp} - \underline{\mathbf{v}}^n\|$. Clearly, the mean model can be considered as a predictive model if this error is sufficiently small. In general, due to data uncertainties and model uncertainties, this error is not sufficiently small and has to be reduced by taking into account data uncertainties and model uncertainties.

3 NONPARAMETRIC PROBABILISTIC APPROACH OF RANDOM UNCERTAINTIES

3.1 *Nonparametric probabilistic approach of random uncertainties*

Poor predictions from predictive models of complex systems are mainly due to model uncertainties. To reduce model uncertainties, a smaller spatial scale can be added to the predictive model. This effort however increases data uncertainties. Today, it is well understood that the parametric probabilistic approach allows data uncertainties to be taken into account in predictive models but not model uncertainties. This is the reason why a nonparametric probabilistic approach is proposed here to take model uncertainties into account.

3.2 *Concept of the nonparametric probabilistic approach to take into account model uncertainties*

The following example will be used to clarify the concepts of the nonparametric approach that permits the consideration of model uncertainty. Let $\mathbf{s} \mapsto A(\mathbf{s})$ be a linear mapping from a space $\mathcal{S}$ into a space $\mathcal{A}$ of linear operators. The space $\mathcal{S}$ represents the set of all possible values of the vector-valued parameter $\mathbf{s}$ of the boundary value problem (for instance, geometric parameters, elastic properties, boundary conditions, etc). For $\mathbf{s}$ fixed in $\mathcal{S}$, operator $A(\mathbf{s})$ represents one operator of the boundary value problem (for instance, the stiffness operator which is assumed to be symmetric and positive, and in this case, any operator in $\mathcal{A}$ will be symmetric and positive). Let $R_{\text{par}} \subset \mathcal{A}$ be the range of the mapping $\mathbf{s} \mapsto A(\mathbf{s})$, i.e. the subset of $\mathcal{A}$ spanned by $A(\mathbf{s})$ when $\mathbf{s}$ runs through $\mathcal{S}$.

(A) *The operator of the real system*. It is assumed that the operator corresponding to the real system is $\mathbf{A}^{\exp}$ belonging to $\mathcal{A}$.

(B) *The mean model of the operator*. If $\mathbf{s} = \underline{\mathbf{s}}$ is the nominal value, then $\underline{A} = A(\underline{\mathbf{s}}) \in R_{\text{par}}$ is the operator of the mean model.

(C) *Parametric probabilistic model of the operator*. The parametric probabilistic approach for the operator consists in modeling the parameter $\mathbf{s}$ by a vector valued random variable $\mathbf{S}$ whose probability distribution $P_{\mathbf{S}}(d\mathbf{s})$ has a support which is $\mathcal{S}$. Then the operator $\underline{A}$ of the mean model is replaced in the the BVP by the random operator $\mathbf{A}_{\text{par}}$ such that $\mathbf{A}_{\text{par}} = A(\mathbf{S})$. The probability distribution $P_{\mathbf{A}_{\text{par}}}$ of the random operator $\mathbf{A}_{\text{par}}$ is $P_{\mathbf{A}_{\text{par}}} = A(P_{\mathbf{S}})$ and its support is the set $R_{\text{par}} \subset \mathcal{A}$ (see Fig. 2). Clearly, the probability $P_{\mathbf{A}_{\text{par}}}$ on R_{par} allows data uncertainties to be taken into account, but $\mathbf{A}^{\exp}$ may not be in R_{par} due to model uncertainties.

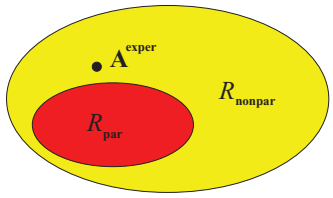

Figure 2. Parametric and nonparametric probabilistic approaches of random uncertainties.

(D) *Nonparametric probabilistic model of the operator*. The nonparametric probabilistic approach for the operator consists in replacing the operator $\underline{A}$ of the mean model by a random operator $\mathbf{A}_{\text{nonpar}}$ whose probability distribution $P_{\mathbf{A}_{\text{nonpar}}}$ has a support $R_{\text{nonpar}} = \mathcal{A}$. Since $\mathbf{A}^{\exp}$ belongs to $\mathcal{A}$ and since the support of $P_{\mathbf{A}_{\text{nonpar}}}$ is also $\mathcal{A}$, model uncertainties can be taken into account by the proposed nonparametric approach (see Fig. 2). Of course, $P_{\mathbf{A}_{\text{nonpar}}}$ cannot be arbitrary chosen with support R_{nonpar}, but has to be constructed using the available information. Such a methodology has been developed (Soize 1999, 2000, 2001a and 2005b) by using the maximum entropy principle (Shannon 1948) and (Jaynes 1957).

3.3 *Evolution of the concepts: some history*

The fundamentals of the nonparametric approach for random uncertainties and the developments of the first ensemble of random matrices adapted to modeling random uncertainties in linear dynamical systems have been introduced by Soize (1999) and (2000). The algebraic closure of this theory and its convergence analysis as the dimension goes to infinity have studied by Soize (2001a) and (2001b) in the context of transient linear elastodynamics of stochastic systems. Others ensembles of random matrices adapted to modeling random uncertainties for coupled systems encountering vibroacoustics problems, have been introduced by Soize (2005b).

The extension of the theory to non homogeneous uncertainties in complex dynamical systems using substructuring techniques can be found, with experimental validations, in Chebli & Soize (2004), Duchereau & Soize (2005).

The identification of the parameters of the nonparametric probabilistic model from experiments is developed in Soize (2005a) and (2005b) and an experimental validation is given in Chen et al. (2004).

The extension of the theory to linear dynamical systems in the medium frequency range was achieved by Soize (2003b). The random eigenvalues for linear dynamical systems and the non adaptation of the Gaussian Orthogonal Ensemble (GOE) for low- and medium-frequency dynamics are analyzed in Soize (2003a).

The application of this nonparametric probabilistic approach for model uncertainties in nonlinear dynamical systems and transient nonlinear dynamics of stochastic systems have been studied in Soize (2001c), Desceliers et al. (2004).

Model uncertainties in dynamical systems with cyclic symmetry and applications to mistuned bladed disks have been developped in Capiez-Lernout & Soize (2004) and Capiez-Lernout et al. (2005b).

Additional validations devoted to the capability of the nonparametric probabilistic approach to take into account model uncertainties is given in Soize (2005a) and Capiez-Lernout et al. (2005b). The extension of the theory to vibroacoustic problems is presented in Durand et al. (2005).

4 METHODOLOGY OF THE NONPARAMETRIC PROBABILISTIC APPROACH FOR RANDOM UNCERTAINTIES

The methodology of the nonparametric probabilistic approach of uncertainties in dynamical systems is as follows.
(1) Developement of a mechanical-mathematical model, generally a finite element model, of the designed system. Such a model will be call the mean model (or the nominal model).
(2) Construction of a reduced mean model from the mean model.
(3) Construction of a stochastic reduced model from the reduced mean model using the nonparametric concept and the maximum entropy principle. In this fashion, the probability distribution of each random generalized matrix is constructed.
(4) Construction and convergence analysis of the stochastic solution.

4.1 *Mean finite element model of the dynamical system*

The following presentation is limited to the nonlinear structural dynamics of a linear structure with localized nonlinearities but it can be extented to other more complex systems such as vibroacoustic systems (see Section 7.4). We consider a nonlinear dynamic system constituted of a three-dimensional, damped, fixed structure vibrating around a static equilibrium configuration considered as a natural state without prestresses. The struvture is subjected to an external load and does not display rigid body displacement. The basic finite element model of this nonlinear dynamic system is called the "mean finite element model" (the underlined quantities refer to this "mean finite element model") and leads to the following nonlinear differential equation,

$$[\underline{\mathbb{M}}]\,\underline{\ddot{\mathbf{y}}}(t) + [\underline{\mathbb{D}}]\,\underline{\dot{\mathbf{y}}}(t) + [\underline{\mathbb{K}}]\,\underline{\mathbf{y}}(t) + \mathbf{f}_{\rm NL}(\underline{\mathbf{y}}(t), \underline{\dot{\mathbf{y}}}(t)) = \mathbf{f}(t)\,, \quad (1)$$

in which $\underline{\mathbf{y}} = (\underline{y}_1, \ldots, \underline{y}_m)$ is the unknown time response vector of the m degrees of freedom (DOF) (displacements and/or rotations); $\underline{\dot{\mathbf{y}}}$ and $\underline{\ddot{\mathbf{y}}}$ are the velocity and acceleration vectors respectively; $\mathbf{f}(t) = (f_1(t), \ldots, f_m(t))$ is the known external load vector of the m inputs (forces and/or moments); $[\underline{\mathbb{M}}]$, $[\underline{\mathbb{D}}]$ and $[\underline{\mathbb{K}}]$ are the mass, damping and stiffness matrices of the linear part of the model, which are positive-definite symmetric $(m \times m)$ real matrices; $(\mathbf{y}, \mathbf{z}) \mapsto \mathbf{f}_{\rm NL}(\mathbf{y}, \mathbf{z})$ is a nonlinear mapping from $\mathbb{R}^m \times \mathbb{R}^m$ into $\mathbb{R}^m$ modeling additional nonlinear damping and restoring forces such that $\mathbf{f}_{\rm NL}(0, 0) = 0$. The linear case can be derived from Eq. (1) by taking $\mathbf{f}_{\rm NL} = 0$.

4.2 *Reduced mean model*

Let $\{\underline{\boldsymbol{\varphi}}_1, \ldots, \underline{\boldsymbol{\varphi}}_m\}$ be an algebraic basis of $\mathbb{R}^m$. The reduced mean model of the dynamic system with mean finite element model given by Eq. (1) is obtained by projection of Eq. (1) on the subspace V_n of $\mathbb{R}^m$ spanned by $\{\underline{\boldsymbol{\varphi}}_1, \ldots, \underline{\boldsymbol{\varphi}}_n\}$ with $n \ll m$.
The construction of such an algebraic basis can be performed as follows.

(1) By using elastic modes of the underlying linear dynamical system. This choice is warranted for linear dynamical systems or for nonlinear dynamical systems with localized nonlinearities, when their responses are in the low-frequency range.

(2) By using eigenvectors of the mechanical energy operator. This solution is appropriate for a linear dynamical system in the medium-frequency range

© 2005 Millpress, Rotterdam, ISBN 90 5966 040 4

(Soize 1998a,1998b,1999,2003b), (Soize & Mziou 2003), (Ghanem & Sarkar 2003).

(3) By using adapted "nonlinear modes" for nonlinear dynamical systems with distributed nonlinearities.

Let $[\underline{\Phi}_n]$ be the $(m \times n)$ real matrix whose columns are the vectors $\{\underline{\varphi}_1, \ldots, \underline{\varphi}_n\}$. The generalized force $\mathbf{F}^n(t)$ is the $\mathbb{R}^n$-vector $\mathbf{F}^n(t) = [\underline{\Phi}_n]^T \mathbf{f}(t)$. The generalized mass, damping and stiffness matrices $[\underline{M}_n]$, $[\underline{D}_n]$ and $[\underline{K}_n]$ are the positive-definite symmetric $(n \times n)$ real matrices $[\underline{M}_n] = [\underline{\Phi}_n]^T [\underline{\mathbb{M}}] [\underline{\Phi}_n]$, $[\underline{D}_n] = [\underline{\Phi}_n]^T [\underline{\mathbb{D}}] [\underline{\Phi}_n]$, and $[\underline{K}_n] = [\underline{\Phi}_n]^T [\underline{\mathbb{K}}] [\underline{\Phi}_n]$ which, in general, are full matrices. Consequently, the reduced mean model of the nonlinear dynamic system, written as the projection $\underline{\mathbf{y}}^n$ of $\underline{\mathbf{y}}$ on V_n, can be written as

$$\underline{\mathbf{y}}^n(t) = [\underline{\Phi}_n]\, \underline{\mathbf{q}}^n(t) \quad , \tag{2}$$

in which the vector $\underline{\mathbf{q}}^n(t) \in \mathbb{R}^n$ of the generalized coordinates satisfies the mean nonlinear differential equation,

$$[\underline{M}_n]\, \underline{\ddot{\mathbf{q}}}^n(t) + [\underline{D}_n]\, \underline{\dot{\mathbf{q}}}^n(t) + [\underline{K}_n]\, \underline{\mathbf{q}}^n(t) + \mathbf{F}^n_{\text{NL}}(\underline{\mathbf{q}}^n(t), \underline{\dot{\mathbf{q}}}^n(t)) = \mathbf{F}^n(t) \ , \ \forall t \geq 0 \ , \tag{3}$$

where, for all $\mathbf{q}$ and $\mathbf{p}$ in $\mathbb{R}^n$,

$$\mathbf{F}^n_{\text{NL}}(\mathbf{q}, \mathbf{p}) = [\underline{\Phi}_n]^T\, \mathbf{f}_{\text{NL}}([\underline{\Phi}_n]\, \mathbf{q}, [\underline{\Phi}_n]\, \mathbf{p}) \quad . \tag{4}$$

4.3 *Stochastic response of the nonlinear dynamical system with the nonparametric probabilistic model of random uncertainties*

The principle of construction of the nonparametric model of random uncertainties for the dynamical system whose mean finite element model is defined by Eq. (1), consists in modeling the generalized mass, damping and stiffness matrices of the reduced mean model (see Eq. (3)) by random matrices $[\mathbf{M}_n]$, $[\mathbf{D}_n]$ and $[\mathbf{K}_n]$. If the nonlinear forces are uncertain, a usual parametric model can be used for these nonlinear forces. In this case, a mixed nonparametric-parametric formulation can easily be constructed.

The stochastic transient response of the nonlinear dynamic system with a nonparametric probabilistic model of random uncertainties, with reduced mean model defined by Eqs. (2)-(4), is the stochastic process $\mathbf{Y}^n(t)$, indexed by $\mathbb{R}^+$, with values in $\mathbb{R}^m$, such that

$$\mathbf{Y}^n(t) = [\underline{\Phi}_n]\, \mathbf{Q}^n(t) \quad . \tag{5}$$

In this equation, the stochastic process $\mathbf{Q}^n(t)$, indexed by $\mathbb{R}^+$, with values in $\mathbb{R}^n$, is such that

$$[\mathbf{M}_n]\, \ddot{\mathbf{Q}}^n(t) + [\mathbf{D}_n]\, \dot{\mathbf{Q}}^n(t) + [\mathbf{K}_n]\, \mathbf{Q}^n(t) + \mathbf{F}^n_{\text{NL}}(\mathbf{Q}^n(t), \dot{\mathbf{Q}}^n(t)) = \mathbf{F}^n(t) \ , \ \forall t \geq 0 \ , \tag{6}$$

with the initial conditions, $\mathbf{Q}^n(0) = 0$ and $\dot{\mathbf{Q}}^n(0) = 0$.

4.4 *Construction of the probability model of the random matrices* $[\mathbf{M}_n], [\mathbf{D}_n], [\mathbf{K}_n]$

The construction of the probability model of random matrices $[\mathbf{M}_n]$, $[\mathbf{D}_n]$ and $[\mathbf{K}_n]$ consists in taking these random matrices in ensemble SE^+ (Soize, 1999,2000,2001a,2001c) whose construction is recalled below.

(1) The random matrices $[\mathbf{M}_n]$, $[\mathbf{D}_n]$ and $[\mathbf{K}_n]$ are defined on the probability space $(\mathcal{A}, \mathcal{T}, \mathcal{P})$, with values in $\mathbb{M}^+_n(\mathbb{R})$.

(2) The mean values of these random matrices are $E\{[\mathbf{M}_n]\} = [\underline{M}_n]$, $E\{[\mathbf{D}_n]\} = [\underline{D}_n]$ and $E\{[\mathbf{K}_n]\} = [\underline{K}_n]$.

(3) These random matrices verify the following inequalities ensuring that Eq. (6) has a second-order stochastic solution, $E\{\|[\mathbf{M}_n]^{-1}\|_F^2\} < +\infty$, $E\{\|[\mathbf{D}_n]^{-1}\|_F^2\} < +\infty$ and $E\{\|[\mathbf{K}_n]^{-1}\|_F^2\} < +\infty$.

(4) The random matrices $[\mathbf{M}_n]$, $[\mathbf{D}_n]$ and $[\mathbf{K}_n]$ are independent (because no available information is given concerning the correlation between these random matrices).

(5) These random matrices can be normalized with respect to their mean values as follows:

$$[\mathbf{M}_n] = [\underline{L}_{M_n}]^T\, [\mathbf{G}_{M_n}]\, [\underline{L}_{M_n}] \quad , \tag{7}$$

$$[\mathbf{D}_n] = [\underline{L}_{D_n}]^T\, [\mathbf{G}_{D_n}]\, [\underline{L}_{D_n}] \quad , \tag{8}$$

$$[\mathbf{K}_n] = [\underline{L}_{K_n}]^T\, [\mathbf{G}_{K_n}]\, [\underline{L}_{K_n}] \quad , \tag{9}$$

in which $[\underline{L}_{M_n}]$, $[\underline{L}_{D_n}]$ and $[\underline{L}_{K_n}]$ are the upper triangular real matrices in $\mathbb{M}_n(\mathbb{R})$ such that $[\underline{M}_n] = [\underline{L}_{M_n}]^T [\underline{L}_{M_n}]$, $[\underline{D}_n] = [\underline{L}_{D_n}]^T [\underline{L}_{D_n}]$ and $[\underline{K}_n] = [\underline{L}_{K_n}]^T [\underline{L}_{K_n}]$. The random matrices $[\mathbf{G}_{M_n}]$, $[\mathbf{G}_{D_n}]$ and $[\mathbf{G}_{K_n}]$ are in the ensemble SG^+ which is defined in Section 4.5.

(6) The of ensemble SG^+ of random matrices is defined as follows.

4.5 *Ensemble* SG^+ *of random matrices*

(A) *Definition of ensemble* SG^+. This ensemble is defined and constructed (Soize 1999,2000,2001a) as the set of random matrices $[\mathbf{G}_n]$, defined on the probability space $(\mathcal{A}, \mathcal{T}, P)$, with values in $\mathbb{M}^+_n(\mathbb{R})$, whose probability distribution is constructed by using the entropy optimization principle (Shannon 1948), (Jaynes 1957), under the constraints (available information):

(1) Any matrix $[\mathbf{G}_n]$ is symmetric positive-definite real random matrix, i.e.

$$[\mathbf{G}_n] \in \mathbb{M}^+_n(\mathbb{R}) \quad \text{a.s} \quad . \tag{10}$$

(2) Any matrix $[\mathbf{G}_n]$ is a second-order random variable, $E\{\|[\mathbf{G}_n]\|^2\} \leq E\{\|[\mathbf{G}_n]\|_F^2\} < +\infty$ and its mean value $[\underline{G}_n]$ is the $(n \times n)$ identity matrix $[I_n]$,

$$E\{[\mathbf{G}_n]\} = [\underline{G}_n] = [I_n] \in \mathbb{M}^+_n(\mathbb{R}) \quad . \tag{11}$$

(3) Any random matrix $[\mathbf{G}_n]$ is such that

$$E\{\ln(\det[\mathbf{G}_n])\} = v \quad \text{with} \quad |v| < +\infty \quad . \tag{12}$$

The constraint defined by Eq. (12) implies the following fundamental property for random matrices in ensemble SG^+,

$$E\{\|[\mathbf{G}_n]^{-1}\|_F^2\} < +\infty \quad . \tag{13}$$

(B) *Dispersion parameter of a random matrix in ensemble* SG^+. Let δ be the real dispersion parameter defined by

$$\delta = \left\{ \frac{E\{\| [\mathbf{G}_n] - [\underline{G}_n] \|_F^2\}}{\| [\underline{G}_n] \|_F^2} \right\}^{1/2} = \left\{ \frac{1}{n} E\{\| [\mathbf{G}_n] - [I_n] \|_F^2\} \right\}^{1/2} \quad . \tag{14}$$

It controls the dispersion of the probability model of random matrix $[\mathbf{G}_n]$ provided that δ is independent of n and such that

$$0 < \delta < \sqrt{(n+1)(n+5)^{-1}} \quad . \tag{15}$$

(C) *Probability distribution of a random matrix in ensemble* SG^+. The probability distribution $P_{[\mathbf{G}_n]}$ of random matrix $[\mathbf{G}_n]$ is defined by a probability density function $[G_n] \mapsto p_{[\mathbf{G}_n]}([G_n])$ from $\mathbb{M}_n^+(\mathbb{R})$ into $\mathbb{R}^+ = [0\,, +\infty[$, with respect to the measure (volume element)

$$\widetilde{d}G_n = 2^{n(n-1)/4} \, \Pi_{1 \leq i \leq j \leq n} \, d[G_n]_{ij} \quad , \tag{16}$$

on the set $\mathbb{M}_n^S(\mathbb{R})$. We then have

$$P_{[\mathbf{G}_n]} = p_{[\mathbf{G}_n]}([G_n]) \; \widetilde{d}G_n \quad , \tag{17}$$

with the normalization condition

$$\int_{\mathbb{M}_n^+(\mathbb{R})} p_{[\mathbf{G}_n]}([G_n]) \; \widetilde{d}G_n = 1 \quad . \tag{18}$$

The probability density function $p_{[\mathbf{G}_n]}([G_n])$ is then written as

$$p_{[\mathbf{G}_n]}([G_n]) = \mathbb{1}_{\mathbb{M}_n^+(\mathbb{R})}([G_n]) \times C_{\mathbf{G}_n} \times \left(\det [G_n]\right)^{(n+1)\frac{(1-\delta^2)}{2\delta^2}} \times \exp\left\{ -\frac{(n+1)}{2\delta^2} \, \mathrm{tr}\, [G_n] \right\} \quad , \tag{19}$$

in which $\mathbb{1}_{\mathbb{M}_n^+(\mathbb{R})}([G_n])$ is equal to 1 if $[G_n] \in \mathbb{M}_n^+(\mathbb{R})$ and is equal to zero if $[G_n] \notin \mathbb{M}_n^+(\mathbb{R})$. Further, the positive constant $C_{\mathbf{G}_n}$ is such that

$$C_{\mathbf{G}_n} = \frac{(2\pi)^{-n(n-1)/4} \, \left(\frac{n+1}{2\delta^2}\right)^{n(n+1)(2\delta^2)^{-1}}}{\left\{ \Pi_{j=1}^n \Gamma\left(\frac{n+1}{2\delta^2} + \frac{1-j}{2}\right) \right\}} \quad , \tag{20}$$

where $\Gamma(z)$ is the gamma function defined for $z > 0$ by $\Gamma(z) = \int_0^{+\infty} t^{z-1} \, e^{-t} \, dt$. Equation (19) shows that $\{[G_n]_{jk}, 1 \leq j \leq k \leq n\}$ are dependent random variables.

(D) *Algebraic representation of a random matrix in ensemble* SG^+. The following algebraic representation of a random matrix $[\mathbf{G}_n]$ of SG^+ allows the formulation of a procedure for the Monte Carlo numerical simulation of random matrix $[\mathbf{G}_n]$. With this procedure, the numerical cost induced by the simulation is a constant that depends on dimension n but that is independent of the dispersion parameter δ. Any random matrix $[\mathbf{G}_n]$ can be written as

$$[\mathbf{G}_n] = [\mathbf{L}_n]^T \, [\mathbf{L}_n] \quad , \tag{21}$$

in which $[\mathbf{L}_n]$ is an upper triangular random matrix with values in $\mathbb{M}_n(\mathbb{R})$ such that:

(1) The random variables $\{[\mathbf{L}_n]_{jj'}, j \leq j'\}$ are independent.

(2) For $j < j'$, real-valued random variable $[\mathbf{L}_n]_{jj'}$ can be written as $[\mathbf{L}_n]_{jj'} = \sigma_n U_{jj'}$ in which $\sigma_n = \delta(n+1)^{-1/2}$ and $U_{jj'}$ is a real-valued Gaussian random variable with zero mean and unit variance.

(3) For $j = j'$, the positive-valued random variable $[\mathbf{L}_n]_{jj}$ can be written as $[\mathbf{L}_n]_{jj} = \sigma_n \sqrt{2V_j}$ in which σ_n is defined above and V_j is a positive-valued gamma random variable with probability density function $p_{V_j}(v)$ with respect to dv

$$p_{V_j}(v) = \mathbb{1}_{\mathbb{R}^+}(v) \frac{1}{\Gamma\left(\frac{n+1}{2\delta^2} + \frac{1-j}{2}\right)} \, v^{\frac{n+1}{2\delta^2} - \frac{1+j}{2}} \, e^{-v} \quad . \tag{22}$$

(E) *Convergence property of a random matrix in ensemble* SG^+ *when dimension goes to infinity*. It can be shown that

$$\forall n \geq 2 \quad , \quad E\{\|[\mathbf{G}_n]^{-1}\|^2\} \leq C_\delta < +\infty \quad , \tag{23}$$

in which C_δ is a positive finite constant that is independent of n but that depends on δ. Equation (23) implies that $n \mapsto E\{\|[\mathbf{G}_n]^{-1}\|^2\}$ is a bounded function from $\{n \geq 2\}$ into $\mathbb{R}^+$.

4.6 *Other ensembles of random matrices*

Five ensembles of random matrices have been developped which are useful for modeling data and model uncertainties in computational mechanics . These ensembles differ from the known ensemble of random matrices, e.g. found in Mehta (1991).

(1) The first ensemble, SG^+, of random matrices has been presented in Section 4.5 and is called the *the normalized positive-definite ensemble*. Then, a random matrix belonging to SG^+ is positive definite almost surely and its mean value is the identity matrix. This ensemble constitutes the main ensemble used for constructing the four other ensembles introduced below. Ensemble SG^+ differs from the GOE and from the other known ensembles of random matrix theory (Soize 2003a).

(2) The second ensemble, SE^+, of random matrices, herein called the *positive-definite ensemble*, has been constructed simultaneously with SG^+ and is used in Section 4.4. A random matrix belonging to SE^+ is positive definite almost surely and its mean value is a given positive-definite matrix. For instance, this ensemble is used for constructing probability model of positive operators such as the mass, damping or stiffness operators of a dynamical system.

(3) The construction of the third ensemble, SE^{+0}, has been introduced in Soize (1999) and is similar to the construction of ensemble SE^+. A random matrix belonging to this ensemble is semipositive definite almost surely instead of being positive definite almost surely. For instance, such an ensemble is useful for modeling uncertainties of the stiffness operator of dynamical systems for which there are rigid body displacement fields.

(4) The fourth ensemble of random matrices is the subset $\mathrm{SE}_{\mathrm{lf}}^+$ of SE^+ introduced in Soize (2005b), constituted of random matrices in SE^+ for which a linear

© 2005 Millpress, Rotterdam, ISBN 90 5966 040 4

form on SE^+ is given. A particular case is the ensemble SE^+_{tr} for which the trace of the random matrix is given. For instance, such an ensemble is useful for modeling uncertainties of the mass operator of a dynamical system for which the spatial distibution of the mass is uncertain but for which the total mass is known.

(5) The fifth ensemble, SE_{inv} , of random matrices, herein called the *the pseudo-inverse ensemble*, is a new ensemble introduced in Soize (2005b), constituted of rectangular random matrices having a mean-square pseudo-inverse. For instance, such an ensemble is useful for modeling uncertainties in the coupling operator between an elastic solid and an acoustic fluid (structural-acoustic system) and is used in the application presented in Section 7.4.

4.7 *Construction and convergence of the stochastic solution*

(A) *Stochastic solution as a second-order stochastic process*. For any $T > 0$, it is proved in Soize (2001a,2001c) that, for all t in $[0\,,T]$, we have $E\{\|\mathbf{Y}^n(t)\|^2\} \leq C_1 < +\infty$ and $E\{\|\dot{\mathbf{Y}}^n(t)\|^2\} \leq C_2 < +\infty$ under reasonable assumptions concerning the nonlinear damping and restoring forces and if $\int_0^T \|\mathbf{f}(t)\|^2 dt < +\infty$. Further, C_1 and C_2 are positive constants that are independent of n and t.

(B) *Construction of the stochastic solution*. The stochastic solution of Eq. (6) is constructed using the Monte Carlo numerical simulation with n_s realizations. For each realization, an implicit step-by-step integration method (Newmark method) is used for solving Eq. (6). The realizations of the random matrix $[\mathbf{A}_n]$, in which $[\mathbf{A}_n]$ represents $[\mathbf{M}_n]$, $[\mathbf{D}_n]$ or $[\mathbf{K}_n]$, are constructed using Section 4.5(D). It should be noted that the numerical cost is low with such a method because Eq. (6) corresponds to a stochastic reduced model with $n \ll m$.

(C) *Convergence analysis*. Using the usual estimation of the mathematical expectation operator E, the convergence with respect to dimension n of the stochastic reduced model and to the number n_s of realizations used in the Monte Carlo numerical method, is studied by constructing the function $(n_s, n) \mapsto \mathrm{Conv}(n_s, n)$ defined by

$$\mathrm{Conv}(n_s,n) = \left\{ \frac{1}{n_s} \sum_{k=1}^{n_s} \int_0^T \|\mathbf{Q}^n(t,\theta_k)\|^2 \, dt \right\}^{1/2} , \qquad (24)$$

in which $\mathbf{Q}^n(t,\theta_1), \ldots, \mathbf{Q}^n(t,\theta_{n_s})$ are n_s realizations of $\mathbf{Q}^n(t)$.

5 NUMERICAL VALIDATION: CAPABILITY OF THE NONPARAMETRIC PROBABILISTIC APPROACH TO TAKE INTO ACCOUNT MODEL UNCERTAINTIES

5.1 *Designed system*

The designed system is a slender cylindrical elastic medium $\underline{\Omega}$ defined in a cartesian co-ordinate system $(Oxyz)$ (see Fig. 3). The cylinder has a rectangular section and dimensions $\underline{h}_1 = 10\,m$, $\underline{h}_2 = 1\,m$ and $\underline{h}_3 = 1.5\,m$. The elastic medium is made of a composite material. This structure is simply supported as shown in Fig. 3. The other parts of the boundary $\partial\underline{\Omega}$ of domain $\underline{\Omega}$ are free.

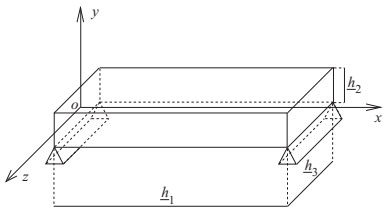

Figure 3. Designed system: linear elastodynamics of a slender three-dimensional elastic medium.

5.2 *Real system*

Figure 4 shows the real system corresponding to the designed system defined in Fig. 3. There are uncertainties on the geometry due to manufacturing tolerances. The domain of the real system is Ω_{RS} which differs from $\underline{\Omega}$. The simply supported conditions are not exactly realized and the composite material does not exactly correspond to the given specifications of the designed system. This real system is excited by a frequency-dependent pressure field $p^{exp}(\omega)$ which is constant in space on the part Γ_{RS} of the boundary $\partial\Omega_{RS}$.

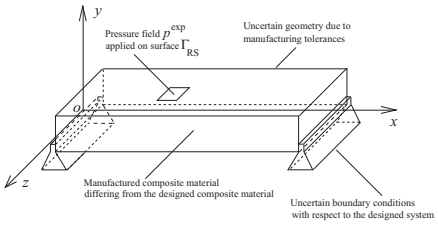

Figure 4. Manufactured system from the designed system defined in Fig. 3.

We are interested in the dynamics of the real system in the frequency band $B =]0,\, 1000]\, Hz$ subjected to a pressure field excitation which is constant in space over Γ_{RS} and constant in frequency band B. The details of data can be found in (Soize, 2005a).

5.3 *Mean model*

The mean model, as a predictive model of the real system defined in Fig. 4, is constructed from the designed system defined in Fig. 3. This mean model is constituted of a damped homogeneous Euler elastic beam with length $\underline{h}_1$, simply supported at $x = 0$ and $x = \underline{h}_1$ (see Fig. 5). The mean model input is the point force located at $x_0 = 4.25\,m$ with an intensity $\underline{g}(\omega) = -\mathbb{1}_B(\omega)$. The composite material of the designed system is modeled by a homogeneous isotropic elastic material whose nominal parameters are $\underline{\mathcal{E}} = 10^{10}\,N/m^2$ (Young's modulus), $\underline{\rho} = 1700\,Kg/m^3$ (mass density) and $\underline{\xi} = 0.01$ (damping rates). The computed eigenfrequencies of the mean system are $\underline{\nu}_1 = 11,\ \underline{\nu}_2 = 44,\ \underline{\nu}_3 = 99,\ \underline{\nu}_4 = 176,\ \underline{\nu}_5 = 275, \underline{\nu}_6 = 396, \underline{\nu}_7 = 539, \underline{\nu}_8 = 704, \underline{\nu}_9 = 891,\ \underline{\nu}_{10} = 1100, \ldots, \underline{\nu}_{80} = 70385\,Hz$. For ω in B, this external force induces flexural vibrations in the plane (Oxy).

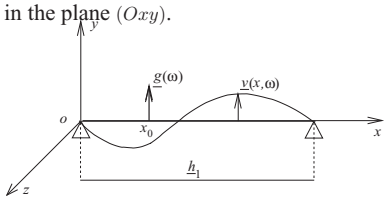

Figure 5. Mean model as the predictive model of the real system resulting from the designed system defined in Fig. 3.

5.4 *Numerical experiment of the real system*

A "numerical experimental" response of the real system is obtained by (1) constructing a 3D elastic model of the real system, (2) discretizing the real system by the finite element method, and (3) solving the equation by modal analysis. The material is taken as homogeneous and isotropic with a Young modulus of $10^{10}\,N/m^2$, a Poisson coefficient of 0.15, a mass density equal to $1700\,Kg/m^3$. The modal damping ratios are the realizations of a uniform random variable on $[0.009\,,0.011]$ of mean value 0.01. The finite element mesh is constituted of $80 \times 8 \times 12 = 7680$ three-dimensional 8-nodes solid elements. There are 9477 nodes and a total of 28275 degrees of freedom (due to the boundary conditions, the displacement is zero for 2×26 nodes). A point force $(0, -\mathbb{1}_B(\omega), 0)$ is applied to the node of co-ordinates $(4.25, 0.5, 0.75)$. The finite element approximation of the displacement field $(u^{\text{exp}}, v^{\text{exp}}, w^{\text{exp}})$ is computed on frequency band B by using modal analysis with the first 150 elastic modes. There are 101 eigenfrequencies in band B and 49 eigenfrequencies in frequency band $[1000, 1197]\,Hz$. The fundamental eigenfrequency is $\nu_1^{\text{exp}} = 16\,Hz$. There are 14 eigenfrequencies in frequency band $[0, 230]\,Hz$. The eigenfrequencies of the first 5 flexural modes corresponding to the first 5 elastic modes of the mean model (Euler beam) and having respectively 2 to 6 nodes (zero Oy-displacement) on the neutral fiber are $\nu_{j_1}^{\text{exp}} = 16,\ \nu_{j_2}^{\text{exp}} = 40,\ \nu_{j_3}^{\text{exp}} = 91,\ \nu_{j_4}^{\text{exp}} = 153,\ \nu_{j_5}^{\text{exp}} = 220,\ Hz$ with $j_1 = 1, j_2 = 3, j_3 = 7, j_4 = 10, j_5 = 14$.

5.5 *Estimation of the dispersion parameters for random uncertainties modeling*

Using the "numerical experiment" of the real system, an estimation of the dispersion parameters δ_M, δ_D and δ_K of the random generalized mass, damping and stiffness matrices is performed by using the method presented in Soize (2003a). Such an estimation yields $\delta_M = 0.29$, $\delta_D = 0.30$ and $\delta_K = 0.68$.

5.6 *Prediction with random uncertainties and "experimental" comparisons*

In this section, we present (1) prediction with the nonparametric probabilistic model of random uncertainties and (2) comparisons with the mean model prediction and with the "experimental" response of the real system. The convergence with respect to n and n_s (dimension of the stochastic reduced model and number of realizations used in the Monte Carlo numerical simulation method) is first studied in Section 4.7. Figure 6 displays the graph of function $n_s \mapsto \text{Conv}(n_s, n)$ defined by Eq. (24) for different values of n. This figure shows that a reasonable convergence is reached for $n \geq 80$ and $n_s \geq 1500$.

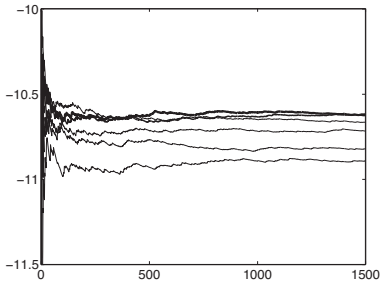

Figure 6. Statistical convergence: graphs of the function $n_s \mapsto \log_{10}\{\text{Conv}(n_s, n)\}$ for $n = 20$, $n = 30$ and 60 (three lower thin solid lines, for $n = 80$, $n = 120$ and $n = 160$ (three upper lines: $n = 80$ (thin solid line), $n = 120$ (mid solid line) and $n = 160$ (thick solid line). Horizontal axis n_s.

Let O_1 and O_2 be the observation points on the line $(x, 0, 0), x \in]0, \underline{h}_1[$ (neutral fiber) and located at $x_1 = 5.000\,m$ and $x_2 = 6.375\,m$ respectively. The confidence region of the modulus of the frequency response function at each observation point O_1 or O_2 is calculated by using the method presented in Section 4. The confidence region for frequency response at a given observation point is carried out with a probability level $P_c = 0.98$ and for $n = 80$ and $n_s = 3000$. For observation points O_1 and O_2, Figs. 7-a and 7-b, respectively, display the comparisons between the mean model response predictions, the "experimental" responses of the real system and the confidence region predictions of the stochastic system resulting from the use of the

© 2005 Millpress, Rotterdam, ISBN 90 5966 040 4

nonparametric probabilistic approach for random uncertainties.

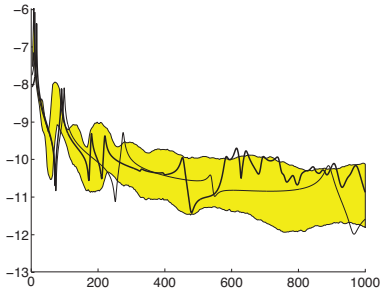

Figure 7-a. Confidence region prediction of the stochastic system with nonparametric approach at observation point O_1 (grey region). Mean model response (thin solid line). "Numerical experiment" of the real system (thick solid line).

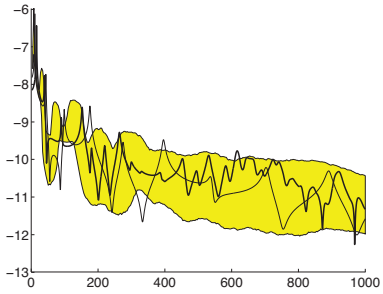

Figure 7-b. Confidence region prediction of the stochastic system with nonparametric approach at observation point O_2 (grey region). Mean model response (thin solid line). "Numerical experiment" of the real system (thick solid line).

5.7 *Lack of capability of the parametric probabilistic approach to take into account model uncertainties*

In this section, we presents the results obtained from the usual parametric probabilistic approach (data uncertainties). For such an approach, the random variables are the mass density ρ, the geometric parameters h_1, h_2 and h_3, the Young modulus $\mathcal{E}$ and the damping ratio ξ. These 6 random variables are assumed to be mutually independent. Positive-valued random variables h_1, h_2 and h_3 are uniformely distributed with known mean values $\underline{h}_1$, $\underline{h}_2$ and $\underline{h}_3$ and coefficients of variation δ_{h_1}, δ_{h_2} and δ_{h_3} to be identified (see below) (the coefficient of variation is the standard deviation divided by the mean value). In addition, it is assumed that $\delta_{h_1} = \delta_{h_2} = \delta_{h_3}$. Positive-valued random variables ρ, $\mathcal{E}$ and ξ are Gamma random variables with known mean values $\underline{\rho}$, $\underline{\mathcal{E}}$ and $\underline{\xi}$ and for coefficients of variation δ_ρ, $\delta_\mathcal{E}$ and δ_ξ to be identified (see below).

Let Λ_1^{par} and $\Lambda_1^{\text{nonpar}}$ be the lowest random eigenfrequencies of the stochastic systems constructed with the parametric and nonparametric approach respectively. Let $\delta_{\Lambda_1^{\text{par}}}$ and $\delta_{\Lambda_1^{\text{nonpar}}}$ be the coefficients of variation of random variables Λ_1^{par} and $\Lambda_1^{\text{nonpar}}$. In order to compare comparable things, the coefficients of variation $\delta_{h_1} = \delta_{h_2} = \delta_{h_3}$, δ_ρ and $\delta_\mathcal{E}$ of random variables h_1, h_2, h_3, ρ and $\mathcal{E}$ for the parametric probabilistic approach, were calculated to yield $\min\{(\delta_{\Lambda_1^{\text{par}}} - \delta_{\Lambda_1^{\text{nonpar}}})^2\}$ in which $\delta_{\Lambda_1^{\text{nonpar}}} = 0.076918$ is known. A solution is $\delta_{h_1} = \delta_{h_2} = \delta_{h_3} = 0.024$, $\delta_\rho = 0.03$, $\delta_\mathcal{E} = 0.1$ corresponding to $\delta_{\Lambda_1^{\text{par}}} = 0.076492$. The coefficient of variation δ_ξ is calculated by the equation $\delta_\xi = \delta_D$ which yields $\delta_\xi = 0.3$.

For observation points O_1 and O_2, Figs. 8-a and 8-b display respectively the comparisons between the mean model response predictions, the "experimental" responses of the real system and the confidence region predictions of the stochastic system resulting from the use of the parametric probabilistic approach of random uncertainties.

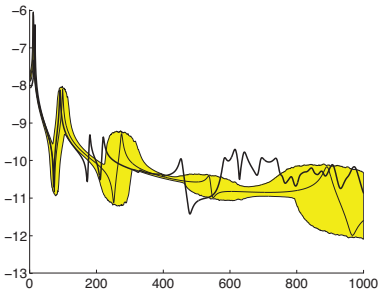

Figure 8-a. Confidence region prediction of the stochastic system with parametric approach at observation point O_1 (grey region). Mean model response (thin solid line). "Numerical experiment" of the real system (thick solid line).

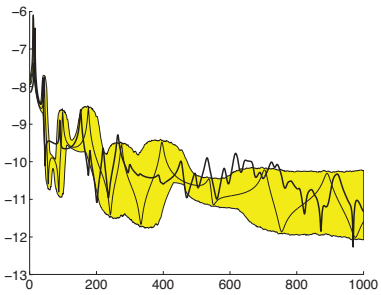

Figure 8-b. Confidence region prediction of the stochastic system with parametric approach at observation point O_2 (grey region). Mean model response (thin solid line). "Numerical experiment" of the real system (thick solid line).

5.8 *Conclusion*

The comparaisons of Fig. 7-a with 8-a and 7-b with 8-b show that the two approaches yield similar results in the low-frequency range $[0\,,100]$ Hz (this band is relatively robust with respect to model uncertainties) are very different in the frequency band $[100, 1000]$ Hz.

The parametric probabilistic approach allows data uncertainties to be taken into account but cannot address model uncertainties which become more significant for frequency increases. On the contrary, the nonparametric probabilistic approach allows model uncertainties to be taken into account.

6 EXPERIMENTAL VALIDATION: NONPARAMETRIC PROBABILISTIC MODEL FOR UNCERTAINTIES IN THE DYNAMICS OF A COMPOSITE SANDWICH PANEL

Two experimental validations of the proposed theory have been published by Chebli & Soize (2004) and Duchereau & Soize (2005) in the context of heterogeneous model uncertainties in vibration and transient dynamics of structures. In this section, we present an experimental validation in another context, i.e. the vibration of multilayer composites. In addition the experimental identification of the dispersion parameters controlling model uncertainties is presented. The details of the results summarized in this section can be found in Chen et al. (2004).

6.1 *Designed panel*

The designed panel is a sandwich panel constituted of five layers four of which are thin carbon-resin unidirectional plies and one is a high stiffness closed-cell foam core (see Fig. 9). This panel is defined with respect to a Cartesian coordinate system $Oxyz$ and is $0.40\,m$ long(Ox axis), $0.30\,m$ wide (Oy axis) and $0.01068\,m$ thick (Oz axis). The middle plane of the sandwich panel is Oxy and the origine O is located in one corner. Each carbon layer is made of a thin carbon-resin ply with a thickness of $0.00017\,m$, a mass density $\rho = 1600\,Kg/m^3$ and whose elasticity constants are: $E_x = 101\,GPa$, $E_y = 6.2\,GPa$, $\nu_{xy} = 0.32$, $G_{xy} = G_{xz} = G_{yz} = 2.4\,GPa$. The first two layers are two carbon-resin unidirectional plies in a [-60/60] layup. The third layer is the closed-cell foam core with a thickness of $0.01\,m$, a mass density of $80\,Kg/m^3$ and elasticity constants: $E_x = E_y = 60\,MPa$, $\nu_{xy} = 0$, $G_{xy} = G_{xz} = G_{yz} = 30\,MPa$. The fourth and fifth layers are two carbon-resin unidirectional plies in a [60/-60] layup.

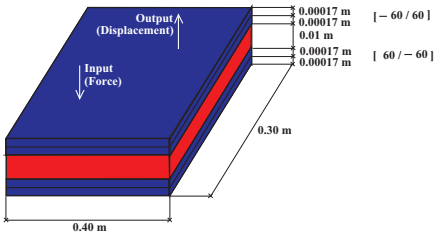

Figure 9. Composite sandwich panel.

6.2 *Experiments*

(A) *Manufactured panels*. Eight sandwich panels were manufactured from the designed panel using the same process and the same materials. All sandwich panels were baked in the same batch to suppress the influence of variations in the baking conditions, e.g. time and temperature.

(B) *Experimental frequency response functions*. The dynamical testing of the eight sandwich panels was realized in the free-free condition. The middle plane of the sandwich panel was vertical and the panel was suspended with a very low eigenfrequency. The measurements were performed on the frequency band $B = [10\,,4500]\,Hz$. The input z-force was a point load applied to point $N0$ of coordinates $(0.187, 0.103, 0)\,m$. An electrodynamic shaker delivered a broad band signal. The output z-accelerations were measured at 25 points by accelerometers. For the sake of brevity, the presentation is limited to the point with coordinates $(0.337, 0.216, 0)\,m$. The experimental cross-frequency response functions were identified on frequency band B using the usual spectral analysis methods and signal processing.

(C) *Experimental modal analysis*. An experimental modal analysis was performed in the frequency band $[10\,,1550]\,Hz$ using the identified experimental frequency response functions. For each sandwich panel $r = 1, \ldots, 8$, eleven elastic modes were identified in this frequency band. For sandwich panel r, the following usual modal parameters of each experimental elastic mode α were identified: (1) the eigenfrequency $\omega_\alpha^{\exp}(\theta_r)$, (2) the damping ratio $\xi_\alpha^{\exp}(\theta_r)$, (3) the elastic mode shape $\psi_\alpha^{\exp}(\theta_r)$ and the corresponding generalized mass $\mu_\alpha^{\exp}(\theta_r)$. Let $\underline{\omega}_\alpha^{\exp} = (1/8)\sum_{r=1}^{8} \omega_\alpha^{\exp}(\theta_r)$ be the average experimental eigenfrequency α. Introducing $\underline{f}_\alpha^{\exp} = \underline{\omega}_\alpha^{\exp}/(2\,\pi)$, the results are $\underline{f}_1^{\exp} = 191.0\,Hz$, $\underline{f}_2^{\exp} = 329.5\,Hz$, $\underline{f}_3^{\exp} = 532.0\,Hz$ and $\underline{f}_4^{\exp} = 635.1\,Hz$. For $\alpha = 1, \ldots, 11$, let $\underline{\xi}_\alpha^{\exp} = (1/8)\sum_{r=1}^{8} \xi_\alpha^{\exp}(\theta_r)$ be the average experimental damping ratio α and let $\underline{\xi}^{\exp} = (1/11)\sum_{\alpha=1}^{11} \underline{\xi}_\alpha^{\exp}$ be the global average experimental damping ratio. The result is $\underline{\xi}^{\exp} = 0.01$.

6.3 *Mean model and its updating*

The designed panel is modeled as a laminated composite thin plate for which each layer is an orthotropic elastic material in plane stress. Since we are only interested in the z-displacement of the middle plane of the sandwich panel in the bending mode and since the panel is a free structure, there are 3 rigid body modes. We are interested in the construction of the responses in the frequency domain over the frequency band of analysis B. The designed panel is modeled by using a regular finite element mesh constituted of 128×64 four-nodes finite elements for laminated plate bending. The number of DOF is $25\,155$. The damping of the structure is introduced by an arbitrary usual model controlled by the modal damping ratios deduced from the measurements. The mean model has

© 2005 Millpress, Rotterdam, ISBN 90 5966 040 4

been updated in average using the first 4 experimental eigenfrequencies for each panel (8 panels).

6.4 *Reduced mean model*

The reduced mean model was constructed by using the first $n = 200$ elastic modes of the updated mean model including the 3 rigid body modes. Convergence was found to be reached for this number of modes.

6.5 *FRF calculation with the reduced mean model and experimental comparisons*

The cross-frequency response function corresponding to the observation point is calcultated with the reduced mean model. Figure 10 displays, in log scale, the graphs of the modulus of the experimental and numerical cross-frequency response functions for which the input is the driven point and the output is the z-acceleration at the observation point. Note that there are 9 curves in the figure: 8 curves correspond to the experimental cross-frequency response functions of the 8 sandwich panels and 1 curve corresponds to the numerical cross-frequency response function computed with the reduced mean model. The comparison of the experimental cross-frequency response functions with the one constructed with the reduced mean model is reasonably good in the frequency band $[0,\, 1500]\, Hz$ and relatively poor in $[1500\,, 4500]\, Hz$. In the frequency band $[1500,\, 4500]\, Hz$, the lack of predictability is increasing with the frequency and is mainly due to model uncertainties (modeling the sandwich panel by using the laminated composite thin plate theory) and to a lesser degree to data uncertainties (mechanical parameters).

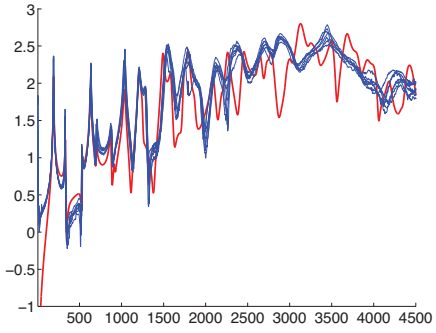

Figure 10. Graphs of the cross-FRF between driven point and observation point. Horizontal axis: frequency in Hertz. Vertical axis: $\log_{10}$ of the modulus of the acceleration in m/s^2. Experimental cross-FRF corresponding to the 8 panels (8 thin solid lines). Numerical cross-FRF calulated with the reduced mean model (thick solid line)

6.6 *Experimental identification of the dispersion parameters of the nonparametric model*

Let δ_M, δ_D and δ_K be the dispersion parameters of the random generalized mass, damping and stiffness matrices. They were estimated by using the experimental generalized matrices corresponding to the 8 experimental sandwich panels, and for a dimension $\nu < n$. The dispersion parameters δ_M, δ_D and δ_K were estimated by (Chen et al. 2004) using the method presented in Soize (2003a and 2005b) and yields $\delta_M = 0.23$, $\delta_D = 0.43$ and $\delta_K = 0.25$ for random matrices $[\mathbf{M}_n]$, $[\mathbf{D}_n]$ and $[\mathbf{K}_n]$ (these values are independent of dimension n of the stochastic reduced model).

6.7 *Confidence region prediction for the FRF and experimental comparisons*

Figure 11 displays the confidence region prediction for the random cross-frequency response functions between the driven point and the observation point, computed with $n_s = 2000$ realizations for the Monte Carlo numerical simulation and $n = 200$ (mean-square convergence is reached for these values).

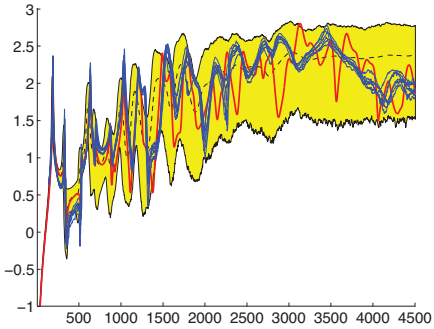

Figure 11. Confidence region prediction for the random cross-FRF. Horizontal axis: frequency in Hertz. Vertical axis: $\log_{10}$ of the modulus of the acceleration in m/s^2. Experimental cross-FRF corresponding to the 8 panels (8 thin solid lines). Numerical cross-FRF calculated with the reduced mean model (thick solid line). Mean value of the random cross-FRF calculated with the nonparametric probabilistic model (thin dashed line). Confidence region of the random cross-FRF calculated with the nonparametric probabilistic model (grey region).

6.8 *Conclusions*

Experimental results obtained for a set of 8 light sandwich panels show the sensitivity of the dynamical response of the panels in the medium-frequency range. The use of the classical laminated composite thin plate theory to construct the predictive mean model introduces significant model uncertainties in the medium-frequency range. Since such dynamical systems are very sensitive to uncertainties, the introduction of a probabilistic model of both data and model uncertainties is necessary to improve the predictability of the mean model. The prediction from the nonparametric model compared with the experiments is good.

7 INDUSTRIAL APPLICATIONS

7.1 *Industrial application 1: Linear dynamics of a bladed disk mistuned by manufacturing uncertainties*

The description of a bladed disk using its cyclic symmetry properties (Thomas, 1979 ; Ohayon & Soize, 1998) is not sufficient to predict accurately its dynamic forced response. In such a mechanical system, there are random uncertainties due to the manufacturing process of the blades. Blade mistuning then refers to the fact that the blades of a bladed disk are slightly different from one to another one. Such a mistuning has significant effects when analyzing the forced response of the bladed disk. It is observed that the vibratory energy of the mistuned bladed disk is localized inducing large dynamic amplification factor (Whitehead (1966), Ewins (1969), Dye & Henry (1969)). Various studies have been carried out to understand and control this phenomenon (see for instance Griffin & Hoosac (1984), Sinha & Chen (1989), Lin & Mignolet (1997), Castanier et al. (1997), Mignolet & Hu (1998), Bladh et al. (2001), Mignolet et al. (2001), Young & Griffin (2001), Petrov et al. (2002), Seinturier et al. (2002)). An exact parametric probabilistic approach would require setting up experimental means to construct a complete probabilistic model of all the parameters related to the random geometry and properties of the blades. Then, functions mapping the domain of uncertain parameters into the mass, damping and stiffness finite element matrices should be constructed. Finally, efficient reduced order models (Bladh et al. (2001), Seinturier et al. (2002)) should be used to analyze the forced response statistics of the bladed disk. It should be noted that such a parametric probabilistic approach would require a large number of uncertain parameters to be experimentally identified in particular for modeling the stochastic fields representing the geometrical and material random uncertainties. An alternative approach based on the use of the nonparametric probabilistic model is proposed and has been used (1) to analyze the direct problem (Capiez-Lernout & Soize, 2004) and (2) to solve the inverse problem consisting in estimating the manufacturing tolerances required so that the random amplification factor of the mistuned disk has a probability level lower than a given value (Capiez-Lernout et al. 2005a). Below, it is shown how the nonparametric probabilistic approach of uncertainties can be used for constructing the probability density function of the amplification factor due to the mistuning. The details concerning this application can be found in Capiez-Lernout et al. (2005a).

(A) *Mean model*. The structure under consideration is a wide chord supersonic fan geometry. The fan has 22 blades. The finite element model of the bladed disk shown in Fig. 12 is constituted of $31\,812$ solid elements and the mean model has $m = 504\,174$ degrees of freedom. Each sector contains 8133 nodes which corresponds to $22\,947$ degrees of freedom. The structure is in rotation around its revolution axis with a constant velocity $\Omega = 4500\,rpm$. The frequency band of analysis for which mistuning effects occur is $B = [515, 535]\,Hz$.

(B) *Reduced mean model*. The mean model of the structure is reduced by the substructuring method introduced by Benfield & Hruda (1971). The efficiency of this method has been proved for mistuned industrial bladed disks with each blade constituting a branch component of the disk substructure. Each blade is reduced by using the Craig & Bampton method (Craig & Bampton 1968). A reduced mean model of the disk with loaded coupling interfaces is constructed by modal analysis. In order to connect the substructures, the displacement of each blade on the coupling interface is projected on the disk modes by using the continuity of displacements at the coupling interface. The reduced mean model is constructed with 660 modes constituted of 10 blade modes per each of the 22 blades (Craig $\&$ Bampton) and 440 modes for the loaded disk (Benfield $\&$ Hruda).

Figure 12. Finite element mesh for the 22 blades fan stage

(C) *Nonparametric probabilistic modeling of uncertainties: probability density function of the random amplification factor due to the mistuning induced by manufacturing tolerances*. Blades uncertainties are due to the blade manufacturing tolerances. The dispersion parameter of the stiffness matrix for each blade is $\delta_K = 0.05$ and has been estimated from the tolerances values (Capiez-Lernout et al., 2005). The stochastic equations are solved with the Monte Carlo numerical simulation method with 1500 realizations and using a heterodyne strategy for computing the random variables in order to accelerate the stochastic convergence. Here, the amplification factor of a blade is relative to its elastic energy. For a given frequency in B, the dynamical amplification factor is defined as the maximum over the 22 blades of the elastic energy of the forced response of each blade for the mistuned

© 2005 Millpress, Rotterdam, ISBN 90 5966 040 4

system, normalized with respect to the tuned system.

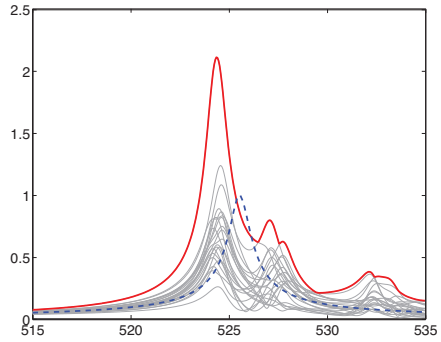

Figure 13. (1) Dynamical amplification factor for the tuned system (dashed line), (2) realization of the random dynamical amplification factor for the mistuned system and for the 22 blades (thin solid lines) and (3) realization of the maximum over the 22 blades of the random dynamical amplification factor for the mistuned system (thick solid line)

Figure 13 displays, versus the frequency in B, the dynamical amplification factor for the tuned system, a realization of the random dynamical amplification factor for each of the 22 blades (for the mistuned system) and the realization corresponding to the maximum over the 22 blades. Figure 14, which is associated with Fig. 13, shows the corresponding spatial localization of the vibrations induced by the mistuning. Figure 15 displays the probability density function of the maximum over band B of the random dynamic amplification factor for the mistuned system.

(D) *Conclusion*. The proposed approach allows the estimation probability density function of the maximum of the random amplification factor due to mistuning, i.e. induced by manufacturing tolerances. The inverse problem which consists in finding the tolerances in order that the maximum of the random dynamical amplification factor be large than a given value with a given probability level is analyzed in (Capiez-Lernout et al. 2005).

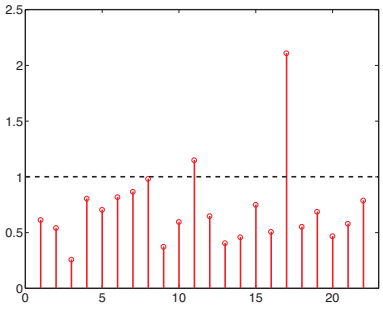

Figure 14. Localized vibrations of the mistuned system. Horizontal axis: blade number. Vertical axis: realization of the random dynamic amplification factor for each blade for the mistuned system and for the frequency for which the maximum is reached.

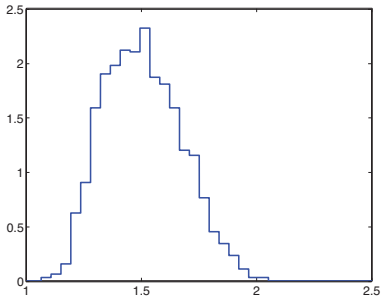

Figure 15. Probability density function of the maximum of the random dynamic amplification factor for the mistuned system.

7.2 *Industrial application 2 : Identification and quantification of the design margins in nonlinear dynamics of a reactor coolant system*

This application deals with model uncertainties for a predictive model in transient nonlinear dynamics of a reactor coolant system (PWR) to identify and quantify the design margins. The nonlinear dynamical system is composed of a linear damped elastic structure representing the reactor cooling system. The nonlinearities are due to restoring forces induced by elastic stops modeling supports of the reactor cooling system. For given gaps, these elastic stops limit the vibration amplitudes of the steam generator system. The displacement field of this structure is constrained by several time-dependent Dirichlet conditions corresponding to seismic loads operating on the anchors of the reactor cooling system and elastic stops. The details of this application can be found in Desceliers et al. (2004).

(A) *Real system*. The real system is a multisupported reactor coolant system inside a building (see Fig. 16) subjected to seismic loads. The structure under consideration (see Fig. 17) is a four-loop reactor coolant system (Duval et al. 1999). Each loop is constituted of a reactor, a reactor coolant pump and a steam generator (see Fig. 18). These three elements are connected to each other by three primary coolant pipes: a hot leg which links the reactor with the steam generator, a cold leg which links the reactor with a reactor coolant pump and an intermediate leg which links the reactor coolant and the steam generator. Its supports consist in anchors located under the reactor coolant pumps, the steam generators and the cold legs. Due to seismic loads, the displacements of all 36 supports are constrained by time-dependent Dirichlet conditions. The vibrations of each steam generator are limited by three elastic stops located at their connection point with the intermediate leg and the hot leg and located at the middle of each steam generator. These elastic stops induce nonlinear restoring forces. In addition, the seven elastic stops are subjected to seismic load and consequently, at each stop, the displacements are

constrained by time-dependent Dirichlet conditions. Excitation is the ground motion due to earthquake which induces accelerations at the supports of the structure constituted of the reactor coolant system.

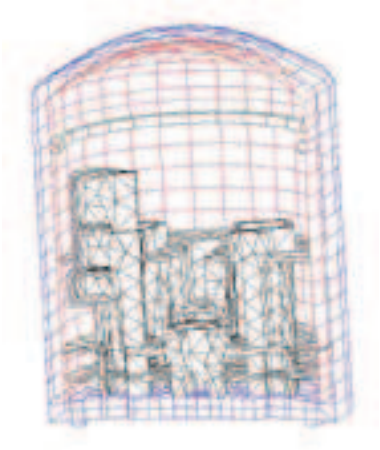

Figure 16. Three-dimensional model of the building containing the reactor coolant system, with soil structure interaction.

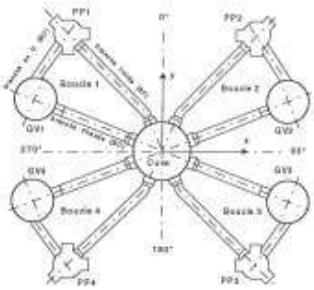

Figure 17. Four loops reactor coolant system.

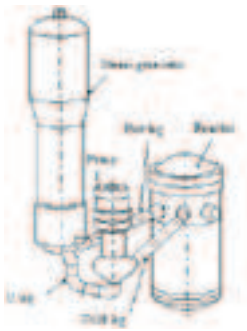

Figure 18. One loop constituted of the reactor, a reactor coolant pump and a steam generator.

(B) *Mean model*. The mean finite element model of the four-loop reactor coolant system is constituted of a curvilinear finite element mesh of a steam generator, of one loop and of the four-loop reactor coolant system as shown in Fig. 19. The structure is multi-supported with 36 supports. The first eigenfrequency of the linear system (without stops) is 1.4 Hz and the eigenfrequency of rank 200 is 164 Hz.

Figure 19. Mean finite element model of the four loops reactor coolant system, constituted of a curvilinear finite element meshes.

The model uncertainties are induced by the introduction of reduced kinetic in the construction of the mean finite element model. For instance, the steam generator (see Fig. 20) is modeled by the curvilinear finite element model shown in the figure.

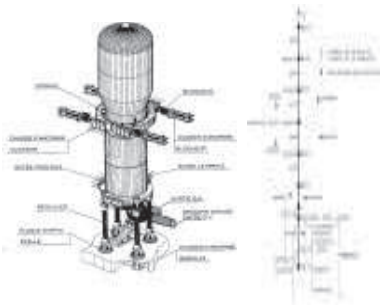

Figure 20. Example of model uncertainties induced by the introduction of a reduced kinematic.

(C) *Reduced mean model*. The structure with fixed supports has no rigid body modes. The transient nonlinear dynamical equation is usually reduced by using the first n structural modes of the associated linear dynamical system with fixed supports and without stops.

(D) *Nonparametric probabilistic modeling of uncertainties: quantification of the design margins of the reactor coolant system*. Model uncertainties and data uncertainties for the linear part of the dynamical system are taken into account with the nonparametric approach for which the dispersions of random generalized mass, damping and stiffness matrices are $\delta_M = \delta_D = \delta_K = 0.2$. Data uncertainties for the nonlinear part (elastic stops) are taken into account with the parametric approach consisting in modeling the stiffness of each stop by a Gamma random variable whose mean value is the value of the mean

© 2005 Millpress, Rotterdam, ISBN 90 5966 040 4

system and for which the dispersion is $\delta = 0.2$ (all 28 elastic stops have the same dispersion). The Monte Carlo numerical simulation is used for obtaining the response of the nonlinear stochastic dynamical system. Since the structure is multisupported and the number of nonlinear elastic stops is large, the solution is very sensitive to the value of the integration time-step size. For the present computations, the time-step Δt was chosen as a constant independent of the dimension n of the stochastic reduced model. For each realizations θ_k of the Monte Carlo numerical simulation , the nonlinear dynamic equations were solved using the Euler explicit step-by-step integration scheme with $\Delta t = 1/25000s$ and for a total time $T = 15s$. A mean-square stochastic convergence analysis has been perfomed with respect to the dimension n of the stochastic reduced model and to the number n_s of realizations used in the Monte Carlo numerical method. Mean-square convergence with respect to n and n_s is obtained for $n = 100$ and $n_s = 280$. The results shown in Fig. 21 correspond to $n = 200$ and $n_s = 700$. This figure displays the confidence region of the Shock Response Spectrum (SRS) at the middle point of one hot leg in the x_3 direction.

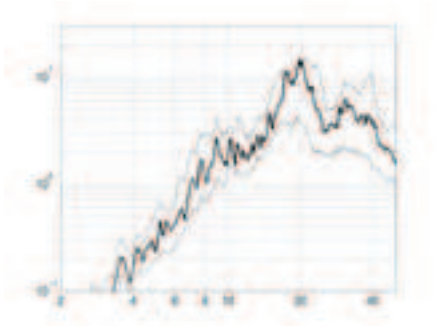

Figure 21. Horizontal axis is the frequency in Hertz. The vertical axis is the pseudo-acceleration spectrum normalized with respect to the gravity acceleration (g=9.91 m/s^2). The thick solid line is the SRS of the mean model and the two thin solid lines are the upper and lower envelopes defining the confidence region for a given probability level equal to 0.98.

(E) *Conclusion*. The construction of the confidence region of the random SRS permits the analysis of the design margins with model uncertainties and data uncertainties. For instance, Fig. 21 shows that the mean model is very robust for the maximum of the response in the frequency band $[17 - 21]$ Hz and less robust in the other part of the frequency band.

7.3 *Industrial application 3: Robustness of the numerical simulation model of a spatial structure with respect to model and data uncertainties in dynamics*

In this section, the robustness of the numerical simulation model of the dynamics of an aerospace structure of Fig. 22 with respect to model and data uncertainties is presented. Data uncertainties are introduced using the parametric probabilistic approach. Model and data uncertainties are also analyzed with the nonparametric probabilistic approach proposed in this paper. A summary of the results is presented below, detail can be found in Capiez-Lernout et al. (2005b) and in Pellissetti (2005).

(A) *Mean model*. The mean finite element model is constructed by subdomains with 5 subdomains: the satellite having 120 000 DOF, the 2 solid propellant boosters 12 000 DOF each, the main stage 8 800 DOF and finally, the upper composite 16 000 DOF. The total finite element model of the aerospace structure has thus 168 800 DOF. The external excitation of the mechanical system is a harmonic driven force applied in the transversal direction (x-axis) to the launcher axis. The frequency band of analysis is $]0\,,60[$ Hz. The observation is the displacement at the end section of the beam connected to the solar panel and is denoted by "obs" in Fig. 23.

(B) *Reduced mean model*. The dynamic substructuring technique (Craig & Bampton, 1968) is used to construct the reduced mean model, each subdomain being a substructure (5 substructures).

(C) *Parametric probabilistic modeling of data uncertainties*. In this application, only the satellite is concerned by data uncertainties. There are 1318 uncertain parameters which are modeled by mutually independent real-valued random variables. The mean value of each random variable is equal to the value of the corresponding parameter of the mean model. The coefficient of variation of each random variable belongs to the range $[0.04\,,0.40]$. Each probability distribution is log-normal or normal depending on the nature of the random parameter which is modeled.

(D) *Nonparametric probabilistic modeling of model and data uncertainties*. The nonparametric approach presented in Section 4 is applied to the reduced mean model of the satellite which is considered as a substructure. Model uncertainties are taken into account for the mass, damping and stiffness operators. The dispersion parameters of the random generalized mass, damping and stiffness matrices related to the satellite substructure are identified using the dispersion of the parametric probabilistic model as follows. Let $\Lambda_1^{\rm par}$ and $\Lambda_1^{\rm nonpar}$ be the lowest random eigenfrequencies of the stochastic system (the satellite in the free-free condition) constructed with the parametric approach and the nonparametric one respectively. The dispersion parameters $\delta_M^{\rm nonpar}$ and $\delta_K^{\rm nonpar}$ of the generalized mass and stiffness random matrices are identified for minimizing the distance between the probability density function of $\Lambda_1^{\rm par}$ and the probability density function of $\Lambda_1^{\rm nonpar}$. The identification of the dispersion parameter $\delta_D^{\rm nonpar}$ for the random generalized damping matrix is performed by minimizing the distance between this random matrix and the corresponding

random matrix constructed with the parametric probabilistic approach. The results of this identification are $\delta_M^{\text{nonpar}} = 0.14$, $\delta_D^{\text{nonpar}} = 0.42$ and $\delta_K^{\text{nonpar}} = 0.13$

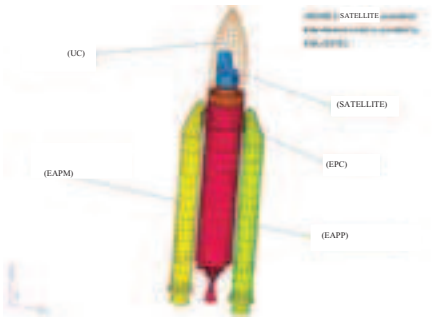

Figure 22. Mean finite element model of the aerospace structure constituted of the statellite coupled with the launcher.

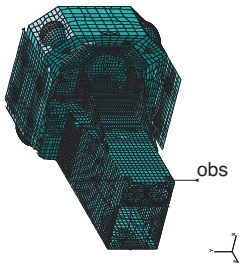

Figure 23. Finite element model of the satellite.

(E) *Robustness of the numerical simulation model with respect to model and data uncertainties*. Figure 24 displays the confidence region of the random displacement for the observation computed with the nonparametric probabilistic approach of model uncertainties and data uncertainties. It can be concluded that the numerical model is robust with respect to model uncertainties and data uncertainties in the low-frequency band [0 , 25] Hertz. The sensitivity of the model to uncertainties increases with the frequency.

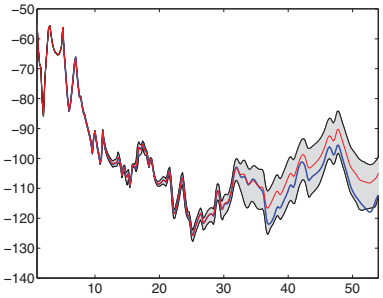

Figure 24. Random displacement for the observation (in dB) calculated with the nonparametric probabilistic approach of model uncertainties and data uncertainties. Response of the mean model (thick solid line). Mean value of the random response(thin solid line). Confidence region for probability level 0.98 (gray region).

The robustness of the numerical model with respect to data uncertainties and model uncertainties can be analyzed from Figs. 25 and 26. Figure 25 displays the displacement for the observation (in dB) which is calculated with the parametric probabilistic approach. It can be seen that the robustness with respect to data uncertainties is not constant in the frequency band [30, 60] Hertz (see Fig. 25), is small in the frequency bands [30, 33] and [45 , 60] Hertz and is larger in the frequency band [33 , 45] Hertz. Figure 26 (which is a zoom of Fig. 24 in the frequency band [30 , 60] Hertz) shows the robustness of the numerical model with respect to model uncertainties and data uncertainties. It can be seen that this robustness decreases with the frequency in the band [30, 60] Hertz. Comparing Figs. 25 and 26, it can be concluded that the numerical model is less robust with respect to model uncertainties than with respect to data uncertainties in the frequency band [30, 60]. Hertz.

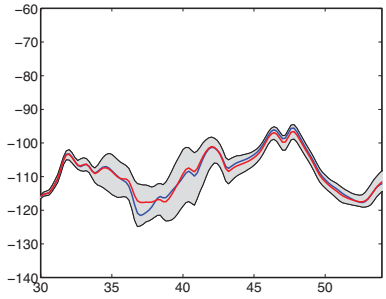

Figure 25. Random displacement for the observed dof (in dB) calculated with the parametric probabilistic approach of data uncertainties. Response of the mean model (thick solid line). Mean value of the random response(thin solid line). Confidence region for probability level 0.98 (gray region).

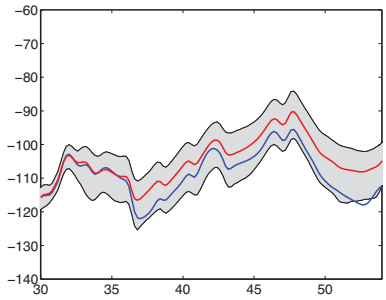

Figure 26. Random displacement for the observed dof (in dB) calculated with the nonparametric probabilistic approach of model uncertainties and data uncertainties. Response of the mean model (thick solid line). Mean value of the random response(thin solid line). Confidence region for probability level 0.98 (gray region).

© 2005 Millpress, Rotterdam, ISBN 90 5966 040 4

7.4 *Industrial application 4: Robustness of numerical vibroacoustic FRF of cars with respect to model and data uncertainties*

The objective of this application is to analyze robustness of numerical vibroacoustic frequency response functions (FRF) of a car with respect to model and data uncertainties. The details concerning the methodology of this application can be found in Durand et al. (2004).

(A) *Mean model of the vibroacoustic system*. The mean finite element model is constructed with 2 subdomains. The first subdomain is the structure (car body) and its finite element model (see Fig. 27) has $1\,132\,356$ degrees of freedon discretizing the displacement field (displacements and rotations). The second subdomain is the internal acoustic cavity and its finite element model (see Fig. 28) has $6\,236$ degrees of freedom (pressure). The two meshes are not compatible on the vibroacoustic coupling interface. The excitation is constituted of forces applied to engine supports (booming noise excitation). The frequency band of analysis is $[1000, 6000]$ rpm (rotation per minute).

Figure 27. Mean finite element of the structure (car body).

Figure 28. Mean finite element model of the internal acoustic cavity with incompatible mesh on the acoustic-structure coupling interface.

(B) *Reduced mean model*. The vibroacoustic equations (mean model) are reduced using the structural modes of the structure (car body) *in vaccuo* and the acoustics modes of the internal acoustic cavity with fixed vibroacoustic coupling interface.

(C) *Nonparametric probabilistic modeling of model and data uncertainties*. The nonparametric probabilistic approach presented in Section 4 is extended to the reduced mean model of the vibroacoustic system. For the structural uncertainties, it is assumed that the levels of uncertainties for the mass, damping and stiffness are the same, which means that $\delta_M^S = \delta_D^S = \delta_K^S$. For the acoustic cavity uncertainties, it is also assumed that the levels of uncertainties for the fluid "mass", "damping" and "stiffness" are the same, which means that $\delta_M^A = \delta_D^A = \delta_K^A$. Finally, for the vibroacoustic coupling uncertainties, the generalized coupling random matrix is modeled using the ensemble of random matrices defined in Section 4.6(5) and for which the uncertainty level is controlled by the parameter δ_C.

(D) *Robustness of the numerical simulation model with respect to model and data uncertainties*. Below, the levels are in dB. In each figure, 1 graduation corresponds to $5\,dB$ on plots. For the structure, the observation is a displacement U with $dB = 20\log_{10}(U)$ and for the internal noise, it is a pressure P with $dB(B) = 20\log_{10}(P/P_0) + B$ in which B is a constant and $P_0 = 2 \times 10^{-5}\,Pa$. For the frequency band of analysis considered, stochastic convergence is reached for 700 structural modes, 50 acoustical modes, and 700 realizations in the Monte Carlo numerical simulation.

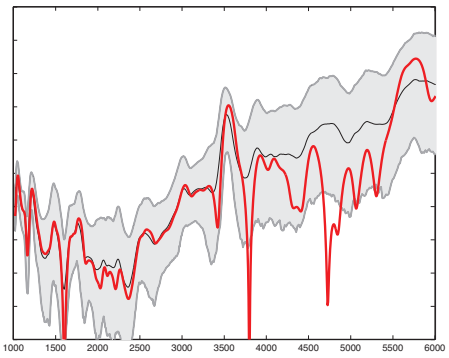

Figure 29. Robustness with respect to structure uncertainties. Normal displacement at the center of a flexible structural element (car roof) in dB. Mean model (thick solid line). Mean value of the random response (thin solid line). Confidence region with probability level 0.95 (gray region). One graduation on the vertical axis corresponds to $5\,dB$.

Figures 29 and 30 are related to the robustness of the structural vibrations of the vibroacoustic system with structural uncertainties (model uncertainties and data uncertainties), without vibroacoustic coupling uncertainties and without acoustic cavity uncertainties. Figure 29 displays the normal displacement at the center of a flexible structural element (car roof)

in dB. The robustness with respect to structure uncertainties is small. Figure 30 displays the normal displacement at the center of a stiff structural element located between the acoustic cavity and the engine. For this structural element, the robustness with respect to structure uncertainties is higher.

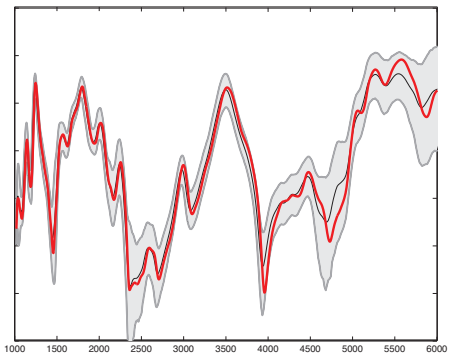

Figure 30. Robustness of the structure response with respect to structure uncertainties. Normal displacement at the center of a stiff structural element in dB. Mean model (thick solid line). Mean value of the random response (thin solid line). Confidence region with probability level 0.95 (gray region). One graduation on the vertical axis corresponds to 5 dB.

Figures 31 and 32 are related to robustness of internal noise for the vibroacoustic system with respect to uncertainties (model uncertainties and data uncertainties). Figure 31 and 32 display the acoustic pressure at the driver ears in dB(B). Figure 31 is related to structure, vibroacoustic coupling and acoustic cavity uncertainties while Fig. 32 is only related to structure uncertainties.

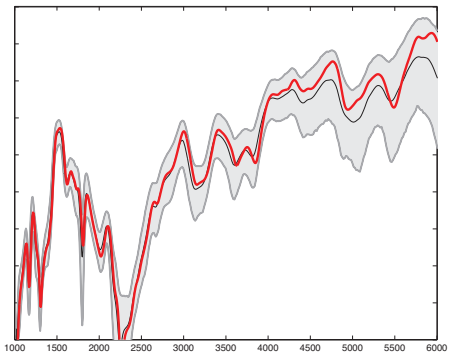

Figure 31. Robustness of the internal noise with respect to structure, vibroacoustic coupling and acoustic cavity uncertainties. Acoustic pressure in dB(B) at the driver ears. Mean model (thick solid line). Mean value of the random response (thin solid line). Confidence region with probability level 0.95 (gray region). One graduation on the vertical axis corresponds to 5 dB.

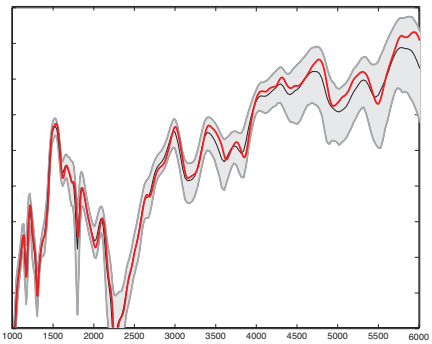

Figure 32. Robustness of the internal noise with respect to structure uncertainties. Acoustic pressure in dB(B) at the driver ears. Mean model (thick solid line). Mean value of the random response (thin solid line). Confidence region with probability level 0.95 (gray region). One graduation on the vertical axis corresponds to 5 dB.

8 CONCLUSIONS

In this paper, a nonparametric probabilistic approach has been proposed to take into account model uncertainties and data uncertainties in computational mechanics. It is shown with a simple example that the usual parametric probabilistic approach allows data uncertainties to be analyzed but does not allow model uncertainties to be taken into account. An additional experimental validation of the approach proposed is given. Four industrial applications in computational mechanics have been presented in different fields showing the interest of such an approach: linear dynamics of a mistuned bladed disk due to manufacturing tolerances, identification and quantification of the design margins in nonlinear dynamics of a reactor coolant system, robustness analysis of the numerical simulation model with respect to model and data uncertainties in dynamics of a spatial structure and finally, robustness analysis of numerical vibroacoustic FRF of cars with respect to model and data uncertainties.

REFERENCES

Benfield, W.A. & Hruda, R.F. 1971. Vibration Analysis of Structures by Component Mode Substitution. *AIAA Journal* Vol. 9(No. 7): 1255-1261.

Bladh ,R., Castanier, M.P. & Pierre,C. 2001. Component-Mode-Based Reduced order Modeling Techniques for Mistuned Bladed Disks-Part 1: Theoretical Models. *Journal of Engineering for Gas Turbines and Power* Vol. 123(No. 1): 89-99.

Capiez-Lernout, E. & Soize, C. 2004. Nonparametric modeling of random uncertainties for dynamic response of mistuned bladed disks. *Journal of Engineering for Gas Turbines and Power* Vol. 126(No. 4): 600-618.

Capiez-Lernout, E., Soize, C., Lombard, J.-P., Dupont, C. & Seinturier, E. 2005a. Blade manufacturing tolerances definition for a mistuned industrial bladed disk. *Journal of Engineering for Gas Turbines and Power* Vol. 127(No. 2).

© 2005 Millpress, Rotterdam, ISBN 90 5966 040 4

Capiez-Lernout, E., Pellissetti, M., Pradlwarter, H., Schuëller, G.I. & Soize, C. 2005b. Data and model uncertainties in complex aerospace engineering systems, *Journal of Sound and Vibration* (submitted in December 2004).

Castanier, M.P., Ottarson, G. & Pierre, C. 1997. A Reduced Order Modeling Technique for Mistuned Bladed Disks. *ASME Journal of Vibration and Acoustics* Vol. 119(No. 3): 439-447.

Chebli, H. & Soize, C. 2004. Experimental validation of a nonparametric probabilistic model of non homogeneous uncertainties for dynamical systems. *J. Acoust. Soc. Am.* Vol. 115(No. 2): 697-705.

Chen, C., Duhamel, D. & Soize, C. 2004. Uncertainties in structural dynamics for composite sandwich panels. *Proceedings of ISMA 2004, the International Conference on Noise and Vibration Engineering, CD-ROM, ISBN 90-73-802-82-2, Katholieke Universiteit Leuven, Belgium, September 20-22, 2004*: 2995-3008.

Chen, P. C. & Soroka, W. W. 1973. Multi-degree dynamic response of a system with statistical properties. *Journal of Sound and Vibration* Vol. 37(No. 4): 547-556.

Craig, R.R. & Bampton, M.M. 1968. Coupling of substructures for dynamical analysis. *AIAA Journal* Vol. 6: 1313-1319.

Desceliers, C., Soize, C. & Cambier, S. 2004. Non-parametric-parametric model for random uncertainties in nonlinear structural dynamics - Application to earthquake engineering. *Earthquake Engineering and Structural Dynamics* Vol. 33(No. 3): 315-327.

Ditlevsen, O. & Tarp-Johansen, N. J. 1998. Choice of input fields in stochastic finite elements. *Probabilistic Engineering Mechanics* Vol. 14(No. 1-2): 63-72.

Duchereau, J. & Soize,C. 2005. Transient dynamics in structures with nonhomogeneous uncertainties induced by complex joints. *Mechanical Systems and Signal Processing*. In press.

Durand, J.-F., Gagliardini, L. & Soize, C. 2004. Random uncertainties for vibroacoustic frequency response functions of cars. *Proceedings of ISMA 2004, the International Conference on Noise and Vibration Engineering, CD-ROM, ISBN 90-73-802-82-2, Katholieke Universiteit Leuven, Belgium, September 20-22, 2004*: 3255-3266.

Duval C, Guyonvarh V, Louche V, Pigat J, Waeckel F. 1999. Estimation methods for seismic behavior of a PWR primary system. *Proceedings of 5th National colloque AFPS*: 19-21.

Dye, R.C.F. & Henry, T.A. 1969. Vibration Amplitudes of Compressor Blades Resulting from Scatter in Blade Natural Frequencies. *ASME Journal of Engineering for Power* Vol. 91(No. 3): 182-187.

Ewins,D.J. 1969. TheeEffects of detuning upon the forced vibrations of bladed disks. *Journal of Sound and Vibration* Vol. 9(No.1): 65-69

Ghanem, R. 1999. Ingredients for a general purpose stochastic finite elements formulation. *Computer Methods in Applied Mechanics and Engineering* Vol. 168: 19-34.

Ghanem, R. & Dham, S. 1998. Stochastic finite element analysis for multiphase flow in heterogeneous porous media. *Transport in Porous Media* Vol. 32: 239-262.

Ghanem, R. & Sarkar, A. 2003. Reduced models for the medium-frequency dynamics of stochastic systems. *Journal of the Acoustical Society of America* Vol. 113(No. 2): 834-846.

Ghanem ,R. G. & Spanos, P. D. 1991. *Stochastic Finite Elements: A Spectral Approach*. New York: Springer-Verlag.

Griffin, J.H. & Hoosac,T.M. 1984. Model development and statistical investigation of turbine blade mistuning. *ASME Journal of Vibration, Acoustics, Stress, and Reliability in Design* Vol.106(No. 2): 204-210.

Haug, E. J., Choi, K. K. & Komkov, V. 1986. *Design Sensitivity Analysis of Structural Systems*. London: Academic Press.

Hien, T. & Kleiber, M. 1997. Stochastic finite element modeling in linear transient heat transfer. *Computer Methods in Applied Mechanics and Engineering* Vol. 144:111-124.

Ibrahim, R. A. 1987. Structural dynamics with parameter uncertainties. *Applied Mechanics Reviews* Vol. 40(No. 3): 309-328.

Iwan, W. D. & Jensen, H. 1993. On the dynamical response of continuous systems including model uncertainty. *Transactions of ASME* Vol. 60: 484-490.

Jaynes, E. T. 1957. Information theory and statistical mechanics. *Physical Review* Vol. 106(No. 4): 620-630 & Vol. 108(No. 2): 171-190.

Jensen, H. & Iwan, W. D. 1992. Response of systems with uncertain parameters to stochastic excitation. *Journal of Engineering Mechanics* Vol. 118(No. 5): 1012-1025.

Kleiber, M., Tran, D. H. & Hien, T. D. 1992. *The Stochastic Finite Element Method*. New York: John Wiley & Sons.

Kotulski, Z. & Sobczyk, K. 1987. Effects of parameter uncertainty on the response of vibratory systems to random excitation. *Journal of Sound and Vibration* Vol. 119(No. 1): 159-171.

Lee, C. & Singh, R. 1994. Analysis of discrete vibratory systems with parameter uncertainties. Part II: Impulse response. *Journal of Sound and Vibration* Vol. 174(No. 3): 395-412.

Le Maître, O. P., Knio, O. M., Najm, H.N. & Ghanem, R. 2001. A stochastic projection method for fluid flow. I. Basic formulation. *Journal of computational Physics* Vol. 173:481-511.

Le Maître, O. P., Knio, O. M., Najm, H.N. & Ghanem, R. 2002. A stochastic projection method for fluid flow. II. Random Process. *Journal of computational Physics* Vol. 181:9-44.

Lin, Y. K. & Cai, G. Q. 1995. *Probabilistic Structural Dynamics*. New York: McGraw-Hill.

Lin, C-C. & Mignolet, M.P. 1997. An adaptative perturbation scheme for the analysis of mistuned bladed disks. *Journal of Engineering for Gas Turbines and Power* Vol. 119(No. 1): 153-160.

Liu, W. K., Belytschko, T. & Mani, A. 1986. Random field finite elements. *International Journal of Numerical Methods in Engineering* Vol. 23: 1832-1845.

Mehta, M. L. 1991. *Random Matrices. Revised and Enlarged Second Edition*. New York: Academic Press.

Micaletti, R. C., Cakmak, A. S., Nielsen, S. R. K. & Koyluglu, H. U. 1998. A solution method for linear and geometrically nonlinear MDOF systems with random properties subject to random excitation. *Probabilistic Engineering Mechanics* Vol. 13(No. 2): 85-95.

Mignolet, M.P. & Hu, W. 1998. Direct prediction of the effects of mistuning on the forced response of bladed disks. *ASME Journal of Engineering for Gas Turbines and Power* Vol. 120(No.3): 626-634.

Mignolet, M.P., Lin, C-C. & LaBorde, B.H. 2001. A novel limit distribution for the analysis of randomly mistuned bladed disks. *Journal of Engineering for Gas Turbines and Power* Vol. 123(No. 2): 388-394.

Ohayon, R. & Soize, C. 1998. *Structural Acoustics and Vibration*. London: Academic Press.

Papadimitriou, C., Katafygiotis, L. S. & Beck, J. L. 1995. Approximate analysis of response variability of uncertain linear systems. *Probabilistic Engineering Mechanics* Vol. 10(No. 4): 251-264.

Pellissitti, M., Capiez-Lernout, E., Pradlwarter, H., Schuëller, G.I. & Soize, C. 2005. Large finite element systems with random uncertainties. *Proceedings 6th International Conference on Structural Dynamics EURODYN 2005, Paris, France, 4-7 September, 2005*.

Petrov, E.P, Sanliturk, K.Y. & Ewins,D.J. 2002. A new method for dynamic analysis of mistuned bladed disks based on the exact relationship between tuned and mistuned systems. *ASME Journal of Engineering for Gas Turbines and Power* Vol. 124(No.3): 586-597.

Pradlwarter, H.J., Schuëller, G.I. & Szekely, G.S. 2002. Random eigenvalue problems for large systems. *Computer and Structures* Vol. 80: 2415-2424.

Prasthofer, P. H. & Beadle, C. W. 1975. Dynamic response of structures with statistical uncertainties in their stiffness. *Journal of Sound and Vibration* Vol. 42(No. 4): 477-493.

Schenk, C.A. & Schuëller, G.I. 2003. Buckling analysis of substructures for dynamic analyses. *Non-Linear Mechanics* Vol. 38: 1119-1132.

Schuëller, G.I. (editor), 1997. A state-of-the-art report on computational stochastic mechanics. *Probabilistic Engineering Mechanics* Vol. 12(No. 4): 197-321.

Schuëller, G.I., Pradlwarter, H.J. & Schenk, C.A. 2003. Non-stationary response of large linear fe-models under stochastic loading. *Computers and Structures* Vol. 81(No. 8-11):937-947.

Seinturier, E., Dupont, C., Berthillier, M. & Dumas, M. 2002. A new aeroelastic model for mistuned bladed disks. *AIAA paper 2002-1533 43rd AIAA/ASME/ASCE/AHS/ASC Structures, Structural Dynamics, and Materials Conference*.

Shannon, C. E. 1948. A mathematical theory of communication. *Bell System Tech. J.* Vol. 27: 379-423 & 623-659.

Shinozuka, M. & Astill, C. J. 1972. Random eigenvalue problems in structural analysis. *AIAA Journal* Vol. 10(No. 4): 456-462.

Shinozuka, M. 1987. Structural response variability. *Journal of Engineering Mechanics - ASCE* Vol. 113(No. 6): 825-842.

Shinozuka, M. & Deodatis, G. 1988. Response variability of stochastic finite element systems. *Journal of Engineering Mechanics* Vol. 114(No. 3): 499-519.

Sinha, A. and Chen, S. 1989. A higher order to compute the statistics of forced response of a mistuned bladed disk assembly. *Journal of Sound and Vibration* Vol. 2(No.130): 207-221.

Soize, C. 1998a. Reduced models in the medium frequency range for general dissipative structural-dynamics systems, *European Journal of Mechanics, A/Solids* Vol. 17(No. 4): 657-685.

Soize, C. 1998b. Reduced models in the medium frequency range for general external structural-acoustics systems, *J. Acoust. Soc. Am.* Vol. 103(No. 6): 3393-3406.

Soize, C. 1999. Reduced models for structures in the medium frequency range coupled with internal acoustic cavities. *J. Acoust. Soc. Am.* Vol. 106(No. 6): 3362-3374.

Soize, C. 1999. A Nonparametric model of random uncertainties in linear structural dynamics. *Publications du LMA-CNRS*, ISBN 2-909669-16-5 Vol. 152: 109-138.

Soize, C. 2000. A nonparametric model of random uncertainties for reduced matrix models in structural dynamics. *Probabilistic Engineering Mechanics* Vol. 15 (No 3): 277-294.

Soize, C. 2001a. Maximum entropy approach for modeling random uncertainties in transient elastodynamics. *J. Acoust. Soc. Am.* Vol. 109 (No. 5): 1979-1996.

Soize, C. 2001b. Transient responses of dynamical systems with random uncertainties. *Probabilistic Engineering Mechanics* Vol. 16(No. 4): 363-372.

Soize, C. 2001c. Nonlinear dynamical systems with nonparametric model of random uncertainties. *Uncertainties in Engineering Mechanics* (e-journal from Resonance Publication, http://www.resonance-pub.com) Vol. 1 (No. 1): 1-38.

Soize, C. 2003a. Random matrix theory and non-parametric model of random uncertainties. *Journal of Sound and Vibration* Vol. 263: 893-916.

Soize, C. 2003b. Uncertain dynamical systems in the medium-frequency range. *Journal of Engineering Mechanics* Vol. 129(No. 9): 1017-1027.

Soize, C. 2004. Random-field model for the elasticity tensor of anisotropic random media. *Comptes Rendus de l'Académie des Sciences - Mécanique* Vol. 332: 1007-1012.

Soize, C. 2005a. A comprehensive overview of a non-parametric probabilistic approach of model uncertainties for predictive models in structural dynamics. *Journal of Sound and Vibration*. In press.

Soize, C. 2005b. Random matrix theory for modeling uncertainties in computational mechanics. *Computer Methods in Applied Mechanics and Engineering* Vol. 194(No. 12-16):1333-1366.

Soize, C. 2005c. Non Gaussian positive-definite matrix-valued random fields for elliptic stochastic partial differential operators, *Computer Methods in Applied Mechanics an Engineering*. In press.

Soize, C. & Chebli H. 2003. Random uncertainties model in dynamic substructuring using a nonparametric probabilistic model. *Journal of Engineering Mechanics* Vol. 129(No. 4): 449-457.

Soize, C. & Ghanem, R. 2004. Physical systems with random uncertainties : Chaos representation with arbitrary probability measure. *SIAM Journal On Scientific Computing* Vol. 26(No. 2): 395-410.

Soize, C. & Mziou, S. 2003. Dynamic substructuring in the medium-frequency range. *AIAA Journal* Vol. 41(No. 6): 1113-1118.

Spanos, P.D. & Ghanem, R.G. 1989. Stochastic finite element expansion for random media. *ASCE Journal of Engineering Mechanics* Vol. 115(No. 5): 1035-1053.

Spanos, P.D. & Zeldin, B.A. 1994. Galerkin sampling method for stochastic mechanics problems. *ASCE Journal of Engineering Mechanics* Vol. 120(No. 5): 1091-1106.

Székely, G.S. & Schuëller, G.I. 2001. Computational procedure for a fast calculation of eigenvectors and eigenvalues of structures with random properties. *Computer Methods in Applied Mechanics and Engineering* Vol. 191: 799-816.

Thomas,D.L. 1979. Dynamics of rotationally periodic structures. *IJNME* Vol. 14 (No. 1): 81-102.

Vanmarcke, E. & Grigoriu, M. 1983. Stochastic finite element analysis of simple beams. *ASCE Journal of Engineering Mechanics* Vol. 109(No. 5): 1203-1214.

Whitehead, D.S. 1966. Effects of mistuning on the vibration of turbomachine blades induced by wakes. *Journal of Mechanical Engineering Science* Vol. 8(No. 1): 15-21.

Yang, M-T. & Griffin, J.H. 2001. A reduced-order model of mistuning using a subset of nominal system modes. *ASME Journal of Engineering for Gas Turbines and Power* Vol. 123(No.3): 893-900.

© 2005 Millpress, Rotterdam, ISBN 90 5966 040 4